DNA-Methylierung und mRNA-Expression von *Tumornekrosefaktor 9* (*4-1BB*) im Malignen Melanom

Detailanalyse der molekularen, immunologischen, pathologischen und klinischen Korrelate

Inaugural-Dissertation

zur Erlangung des Doktorgrades

der Hohen Medizinischen Fakultät

der Rheinischen Friedrich-Wilhelms-Universität

Bonn

Sophia Marie Loick, geb. Walter

aus Wesel

2022

Angefertigt mit der Genehmigung
der Medizinischen Fakultät der Universität Bonn

1. Gutachter: PD Dr. rer. nat. Dimo Dietrich
2. Gutachterin: Prof. Dr. Regina Christine Betz

Tag der Mündlichen Prüfung: 21.09.2022

Aus der Klinik und Poliklinik für Hals-Nasen-Ohren-Heilkunde
Direktor: Prof. Dr. med. Sebastian Strieth

Inhaltsverzeichnis

Abkürzungsverzeichnis

ANOVA	*Analysis of variance;* Varianzanalyse
APC	*Antigen presenting cell*; Antigenpräsentierende Zelle
ARID2	*AT-rich interaction domain 2*; AT-reiches interaktives domänenhaltiges Protein 2
Bcl-xL	*B-cell lymphoma-extra large*
BIM	*Bcl-2-pike protein 11*
CD	*Cluster of differentation*; Cluster der Differenzierung
CTLA4	*Cytotoxic T lymphocyte antigen 4*; zytotoxisches T-Lymphozyten Antigen 4
DNA	*Desoxyribonucleic acid*; Desoxyribonukleinsäure
ERK	*Extracellular signal-regulated kinase;* Extrazellulär geregelte Kinase
H&E	*Hematoxylin and eosin;* Hämatoxylin und Eosin
HNSCC	*Head and neck squamous cell carcinoma*; Kopf- und Hals-Plattenepithelkarzinom
HPV	*Human papillomavirus*; Humanes Papillomavirus
IDH1	Isocitratdehydrogenase 1

IL	Interleukin
IFN	Interferon
JNK	*c-Jun N-terminal kinase;* c-Jun-N-terminale Kinase
mAb	*Monoclonal antibody*; Monoklonaler Antikörper
MAPK	*Mitogen-activated protein kinase;* Mitogen-aktivierte Proteinkinase
mRNA	*Messenger ribonucleic aci*d; Messenger-Ribonukleinsäure
NKC	*Natural killer cell;* Natürliche Killerzelle
PBMC	*Peripheral blood mononuclear cell;* Periphere mononukleäre Blutzellen
PCR	*Polymerase chain reaction;* Polymerasekettenreaktion
PD-1	*Programmed cell death protein 1*
PD-L1	*Programmed cell death ligand 1*
PFS	*Progression-free survival;* Progressionsfreies Überleben
qMSP	*Quantitative methylation specific PCR;* Quantitative methylierungsspezifische PCR
SKCM	*Skin cutaneous melanoma;* Malignes Melanom der Haut
TCGA	*The Cancer Genome Atlas*

TPM	*Transcripts per million;* Transkripte pro Kilobase Exon-Modell pro Million zugeordneter Lesevorgänge
TIL	*Tumor-infiltrating lymphocytes;* Tumorinfiltrierende Lymphozyten
TNF	*Tumor necrosis factor;* Tumornekrosefaktor
TNFRSF	*Tumor necrosis factor receptor superfamily*; Tumornekrosefaktorrezeptor-Superfamilie
TRAF	*TNF receptor associated factors;* TNF-Rezeptor assoziierte Proteine
UHB/UKB	*University Hospital Bonn;* Universitätsklinikum Bonn

1. Deutsche Zusammenfassung

1.1 Einleitung

1.1.1 Immuntherapie und Biomarker

Die Immuntherapie hat sich in den letzten Jahren als wichtige Therapiesäule fortgeschrittener Krebserkrankungen etabliert. Grundlage hierfür ist die Antikörper-vermittelte Aktivierung des patienteneigenen Immunsystems, um eine therapeutisch wirksame Antitumorantwort zu induzieren. Im klinischen Alltag werden beispielsweise sogenannte „Immuncheckpoint-Inhibitoren“ angewandt. Sie sind gegen immuninhibitorische Moleküle wie das *Cytotoxic T lymphocyte antigen 4* (CTLA4), das *Programmed cell death protein 1* (PD-1) oder den *Programmed cell death ligand 1* (PD-L1) gerichtet und werden unter anderem in der Therapie von Melanomen des Stadiums IV verwendet (Deutsche Krebsgesellschaft und Deutsche Krebshilfe AWMF, 2019). Die Immuncheckpoint-Rezeptoren CTLA-4 und PD-1 beweisen die prinzipielle Durchführbarkeit dieser Art von Immuntherapie. Die Blockade von PD-1 wirkt jedoch häufig nur dann, wenn die Tumorzellen den PD-L1 Liganden exprimieren (Yi et al., 2018). Das erklärt teilweise die recht geringen Ansprechraten der aktuell zur Verfügung stehenden Immuntherapeutika von etwa 30% (Schadendorf, 2015). Angesichts der Tatsache, dass nicht alle Patienten gleichermaßen auf verschiedene Immuntherapeutika reagieren, ist es zum einen wichtig, weitere Checkpoint-Rezeptoren zu identifizieren, um alternative Therapiestrategien zur Stärkung der Antitumorimmunität und Verbesserung der Ansprechrate bei Patienten fortgeschrittener maligner Erkrankungen anbieten zu können, und zum anderen sogenannte prädiktive Biomarker zu entwickeln. Dabei stellt neben inhibitorischen Immunregulatoren auch das Mitglied 9 der Tumornekrosefaktorrezeptor-Superfamilie (TNFRSF9; auch 4-1BB oder CD137 genannt) als aktivierender Rezeptor ein vielversprechendes Zielmolekül dar (Ye et al., 2014).

Prädiktive Biomarker sind messbare Parameter, anhand derer möglichst akkurat der Behandlungserfolg vorhergesagt werden kann. Sie können bei der Risikostratifizierung und Auswahl bestmöglicher Therapien helfen. Bisher bekannte, jedoch ungenügend leistungsstarke, Biomarker für gegen PD-1 gerichtete Immuncheckpoint-Modulatoren umfassen die $CD8^+$ T-Zell Infiltration, die Mutationslast und die Expression des

Oberflächenproteins PD-L1 (Topalian et al., 2016). Um die Entwicklung potenterer Biomarker zu ermöglichen, ist ein detailliertes Wissen über epigenetische Regulationsmechanismen von Immuncheckpoint-Genen von großer Wichtigkeit. Die DNA-Methylierung ist ein wichtiger epigenetischer Regulationsmechanismus und könnte somit ein vielversprechender Kandidat eines neuen Biomarkers sein (Pan et al., 2018). Viele Studien belegen eine aberrante Methylierung inhibitorischer Immuncheckpoint-Gene bei diversen malignen Erkrankungen (Chen et al., 2017; Ghoneim et al., 2017; Scharer et al., 2013; Wu et al., 2019). Auch bei Patienten mit metastasiertem Melanom kann beispielsweise die *CTLA4*-Methylierung als prädiktiver Biomarker für Anti-PD-1- und Anti-CTLA-4-Antikörper dienen (Goltz et al., 2018).

1.1.2 TNFRSF9

TNFRSF9 ist ein 255 Aminosäuren umfassendes Typ I-Transmembran-Glykoprotein und Mitglied der Tumornekrosefaktorrezeptor-Superfamilie (TNFRSF) (Schwarz et al., 1993). Als kostimulatorisches T-Zell-Molekül wird es auf aktivierten T-Zellen und natürlichen Killerzellen (NK Zellen) stark, auf Monozyten, Neutrophilen und Dendritischen Zellen konstitutiv auf niedrigerem Niveau exprimiert (DeBenedette et al., 1995; Hurtado et al., 1995). Die *TNFRFS9*-Expression wurde schon mehrfach als potenzieller Biomarker für tumorinfiltrierende Leukozyten (TILs) beim Ovarialkarzinom und beim Malignen Melanom vorgeschlagen (Ye et al., 2014). TNFRSF9 findet man ferner auf Endothelzellen und Tumorkapillaren, insbesondere im entzündeten oder hypoxischen Zustand aber auch bei Morbus Crohn und Rheumatoider Arthritis (Jung et al., 2004; Maerten et al., 2004; Palazon et al., 2011; Palazon et al., 2012). Der TNFSF9-Ligand (auch CD137L oder 4-1BBL genannt) wird auf aktivierten B-Zellen, Dendritischen Zellen, Makrophagen und aktivierten T-Zellen exprimiert (Armitage, 1994; Croft, 2003; Kang et al., 2007). Die Bindung von TNFRSF9 an seinen Liganden oder alternativ an einen agonistischen monoklonalen Antikörper (mAb) induziert die Rekrutierung spezifischer TNF-Rezeptor-assoziierter Faktoren (TRAF1, TRAF2 und TRAF3) (Clark und Ledbetter, 1986). Durch die Interaktion mit TRAF-Proteinen wird mittels 4-1BB wiederum der NF-kB-Signalweg, die Mitogen-aktivierte Proteinkinase (MAPK)-Kaskade, weitere T-Zell-Signalwege (ERK, JNK und p38 MAPK), die Hochregulation der antiapoptotischen Bcl-xL-Familie und die

Hemmung des pro-apoptotischen Proteins BIM aktiviert (Hurtado et al., 1997; Labiano et al., 2017; Maus et al., 2002). So wird in $CD8^+$ T-Zellen der aktivierungsinduzierte Zelltod verhindert und konsekutiv ein besseres Überleben der Zelle gewährleistet (Lee et al., 2002; Schwarz et al., 1993). Ferner kommt es zur Aktivierung, Proliferation, Differenzierung und Freisetzung von Zytokinen, Interleukin 2 (IL-2) und Interferon-Gamma (IFNγ) (Lynch, 2008; Segal et al., 2008). Diese Mechanismen machen TNFRSF9 zu einem attraktiven immuntherapeutischen Ziel. Die vereinfachte Wirkungsweise von TNFRSF9 illustriert Abbildung 1.

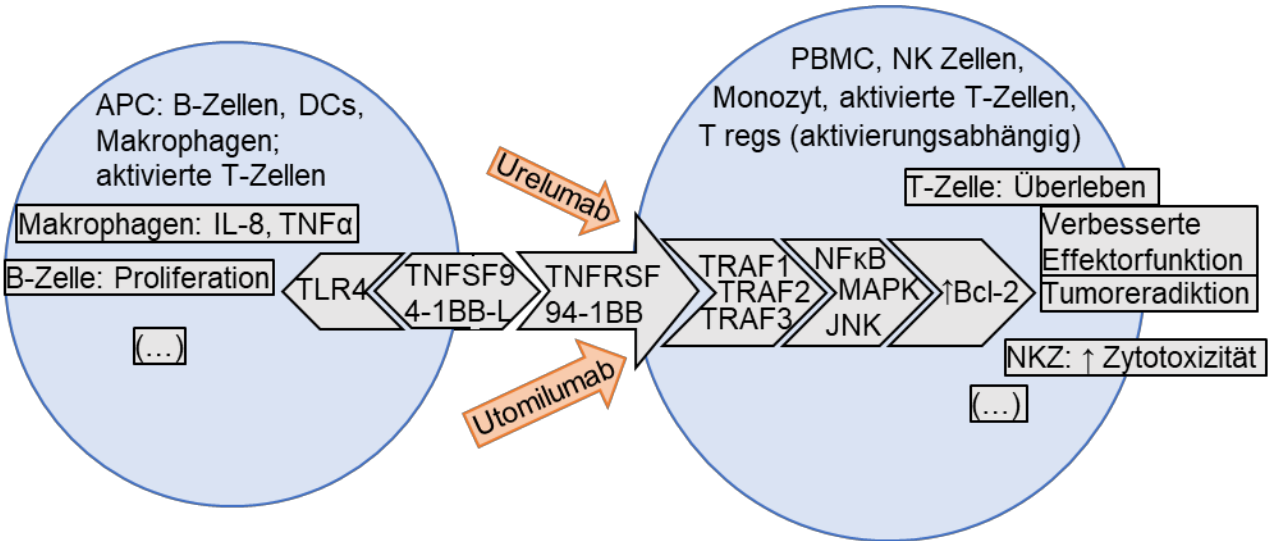

Abb. 1: TNFRSF9 Funktion. Vereinfachte schematische Darstellung der Funktionsweise von TNFRSF9.

In Maus-Tumormodellen haben agonistische TNFRSF9-Antikörper bereits eine stark antitumoröse Wirkung gezeigt. So regressierte das Tumorwachstum in Sarkom-, Gliom- und Lymphom-Modellen (Hurtado et al., 1997; Labiano et al., 2017; Maus et al., 2002). Gleiches konnte präklinisch in Melanomen von Weigelin et al. nachgewiesen werden (Weigelin et al., 2015). Auf Grundlage dieser Ergebnisse werden die zwei agonistischen monoklonalen TNFRSF9-Antikörper, Urelumab (Bristol-Myers Squibb, NY, USA) und Utomilumab (Pfizer, NY, USA), derzeit in diversen klinischen Studien getestet.

1.2 Fragestellung und Zielsetzung

Ziel unserer Studie war es, den Methylierungsstatus des TNFRSF9-kodierenden Gens zu analysieren und so seine Tauglichkeit als prädiktiver Biomarker für das Maligne Melanom zu testen. Zu diesem Zweck haben wir die Korrelate der Methylierung ausgewählter CpG-Dinukleotide des *TNFRSF9*-Gens im Zusammenhang mit der Transkriptionsaktivität (mRNA-Expression), klinischen und pathologischen Parametern, molekularen Eigenschaften, Immunkorrelaten, dem Ansprechen auf eine durchgeführte Anti-PD-1-Immuntherapie und dem progressionsfreien Überleben (PFS) analysiert.

1.3 Material und Methoden

1.3.1 Patientenproben

Für die Analysen haben wir Patienten- und Tumordaten verschiedener Kohorten hinzugezogen:

- TCGA-Kohorte: *N* = 470 Proben des kutanen Malignen Melanoms (SKCM) aus dem *The Cancer Genome Atlas* (TCGA, http://cancergenome.nih.gov/). Unter anderem werden in der TCGA Datenbank Informationen zu klinischen und pathologischen Eigenschaften, zu infiltrierenden Lymphozyten (Verteilung, Dichte und Score), zur UV-Signatur, Mutationslast, Tumorzelldichte und zu spezifischen Mutationsstatus (u.a. *BRAF*) zur Verfügung gestellt. Das TCGA Research Network erhielt die Einverständniserklärung aller Patienten gemäß den Kriterien der Helsinki-Deklaration von 1975.

- UKB Validierungskohorte: *N* = 115 Proben von Melanompatienten des Universitätsklinikums Bonn (UKB), die bisher keine systemische Antitumortherapie erhalten hatten, umfasst diese Kohorte. Es wurde Gewebe aus Primärtumoren, subkutanen und kutanen Metastasen und Lymphknotenmetastasen eingeschlossen. Unsere Studie wurde von der Ethikkommission des Universitätsklinikums Bonn genehmigt.

- Anti-PD1-behandelte Patienten und mRNA ICB Kohorte): *N* = 48 Tumorproben einer Fall-Kontroll-Studie mit Patienten des UKB (UKB ICB Kohorte); hiervon sprachen *N* = 29 auf die Therapie an, bei *N* = 19 kam es zum Fortschreiten der Erkrankung. Dieser Teil der Studie wurde ebenfalls von der Ethikkommission des UKB genehmigt. Zusätzlich *TNFRSF9*-mRNA-Level von *N* = 121 Anti-PD-1-behandelten Patienten (mRNA ICB Kohorte) aus einer jüngst publizierten Arbeit von Liu et al. (2019).
- Zelllinien und Immunzellen: Die Daten primärer Melanozyten- (*N* = 8) und Melanomzelllinien (*N* = 44) wurden der Gene Expression Omnibus (GEO)-Datenbank entnommen (Barrett et al., 2012; Edgar et al., 2002). Die Daten isolierter Leukozyten entstammten bereits veröffentlichten Datensätzen (Absher et al., 2013; Mamrut et al., 2015; Ventham et al., 2016; Zhu et al., 2016). Periphere Mononukleäre Blutzellen (PBMC) *N* = 54, Monozyten *N* = 52, B-Zellen *N* = 60, $CD8^+$ T-Zellen *N* = 28, und $CD4^+$ T-Zellen *N* = 54) sind der GEO Datenbank entnommen (GEO-Akzessionen: GSE44662, GSE122909 und GSE82218, GSE71245, GSE87650, GSE59250).

1.3.2 Probenaufarbeitung

Bisulfit-konvertierte DNA wurde aus Schnitten Formalin-fixierter und Paraffin-eingebetteter Tumorgewebeproben gewonnen. Dazu wurden Tumorareale von auf Glasobjetträgern aufgezogenen Gewebeschnitten mit einem Skalpell makrodisseziert. Die Gewebelyse, die DNA-Denaturierung und die anschließende Bisulfitkonvertierung der DNA führten wir unter Verwendung und gemäß der Herstellerangaben des innuCONVERT Bisulfit All-In-One-Kits (Analytik Jena, Jena, Deutschland) durch. Histopathologisch quantifizierten wir den Leukozyten- und Tumorzellgehalt sowie den Lymphozytenscore anhand von Hämatoxylin-Eosin (HE) Schnitten.

1.3.3 Methylierungsanalyse

Daten zur Genmethylierung vom TCGA Research Network waren von *N* = 470 Melanomproben verfügbar und wurden vom TCGA Research Network mittels des Infinium

HumanMethylation450 BeadChip (Illumina, Inc., San Diego, CA, USA) erhoben. Die DNA-Methylierung der Zelllinien wurde ebenfalls mit dem Infinium HumanMethylation450K gemessen. Die Methylierung der UKB ICB Kohorte wurde mittels des Illumina Infinium MethylationEPIC BeadChip (Illumina, Inc.) bestimmt. Diese Analyse wurde in unserem Auftrag von NXT-Dx (Gent, Belgien) durchgeführt. Von den beiden Illumina Infinium Arrays wurden zwölf Sonden, die auf CpGs innerhalb des *TNFRSF9*-Gens abzielten (Abbildung 2), im Rahmen dieser Arbeit analysiert: cg16839093 (1), cg27305704 (2), cg18859763 (3), cg07836592 (4), cg23959705 (5), cg06956444 (6), cg14614416 (7), cg18025409 (8), cg14153654 (9), cg08840010 (10), cg17123655 (11), cg16117781 (12).

Die Analyse der *TNFRSF9*-Promotormethylierung am CpG-Dinukleotid sechs in Melanomen der Universitätsklinik Bonn (UKB Validierungskohorte) wurde mittels einer quantitativen methylierungsspezifischen Echtzeit-PCR durchgeführt (Vorwärtsprimer: actccataatcactataatacaataa, Rückwärtsprimer: gtagtgtatttttgatgtttggta, $Sonde_{methyliert}$: 6-FAM-ccattacttaaacacaaccgata-BHQ-1, $Sonde_{unmethyliert}$: HEX-accattacttaaacacaaccaatat-BHQ-1). Die PCR wurde in 20 µl Volumen Pufferlösung, 0.4 µM beider Primer und 0.2 µM jeder Sonde durchgeführt. Für den qMSP-Assay verwendeten wir das 7900HT Fast Real-Time PCR System (Biosystems, Waltham, MA, USA) mit dem folgenden Temperaturprofil: 600 s bei 95 °C und 40 Zyklen zu jeweils 15 s bei 95°C, 2 s bei 62 °C und 60 s bei 52 °C. Wir berechneten die prozentualen Methylierungsniveaus unter Verwendung von Zyklusschwellenwerten (CT). Diese wurden mittels Sonden, die spezifisch an Bisulfit umgewandelte methylierte bzw. unmethylierte DNA binden, bestimmt (Methylierung [%] = $100\% / (1 + 2^{CT_{methyliert} - CT_{unmethyliert}})$.

1.3.4 mRNA-Expressionsanalyse

Die mRNA-Expressionsanalysen basieren auf Daten des TCGA Research Network (http://cancergenome.nih.gov/) und wurden vom TCGA Research Network mittels der Illumina HiSeq 2000 RNA Sequencing Version 2 Technologie (Illumina, Inc.) ermittelt. Expressionsdaten der *TNFRSF9*-mRNA waren von *N* = 468 Melanomproben verfügbar.

1.3.5 Immunzellinfiltrate

Als Grundlage der Leukozytenfraktion der Tumorproben verwendeten wir Daten des TCGA Research Networks (Lymphozytenverteilung 0-3, Lymphozytendichte 0-3 und Lymphozytenscore 0-6), die Ausarbeitung von Saltz et al. und additiv Analysen von Thorsson et al. (Saltz et al., 2018; Thorsson et al., 2018). Thorsson et al. und Saltz et al. verwendeten Daten aus DNA-Methylierungsarrays, um die reine Leukozytenfraktion zu identifizieren und RNASeq-Signaturen als Schätzungen für unterschiedliche Immunzellinfiltrate (berechnet mittels CIBERSORT-Algorithmus). So erhielten wir Daten zu folgenden Leukozytenentitäten: $CD8^+$T-Zellen, regulatorische T-Zellen (T reg), follikuläre T-Helferzellen, naïve $CD4^+$T-Zellen, Gedächtnis-$CD4^+$ T-Zellen (ruhend und aktiviert), naive B-Zellen, Gedächtnis-B-Zellen, Plasmazellen, NK Zellen (ruhend und aktiviert), Monozyten und Makrophagen (M0, M1, M2), dendritische Zellen (ruhende und aktiviert), Mastzellen (ruhend und aktiviert), Eosinophile und Neutrophile.

1.3.6 Statistik

Statistische Berechnungen wurden mit SPSS, Version 23.0. (SPSS Inc., Chicago, IL, USA) durchgeführt. Zur Korrelationsberechnung haben wir den Spearman Rangkorrelationskoeffizienten (*Spearman´s ρ*) bestimmt. Die Mittelwerte wurden mit Wilcoxon–Mann–Whitney *U* (zwei Gruppen) und Kruskal–Wallis (>2 Gruppen) Tests verglichen. Um mehrere Vergleiche zwischen Gruppen durchzuführen, wurden One-way ANOVA und post-hoc Bonferroni Tests angewandt. Zur Untersuchung des Überlebens wurden Kaplan-Meier-Analysen und das Regressionsmodell nach Cox verwendet. Für die Kaplan-Meyer-Überlebenskurven wurden die Daten anhand der Methylierungslevel und der mRNA-Expression mittels eines optimierten Schwellenwerts dichotomisiert. Die Schwellenwertoptimierung erfolgte derart, dass die beiden resultierenden Gruppen den größtmöglichen Überlebensunterschied zeigten (kleinster *P*-Wert). Zur Berechnung der Cox Regression wurden die mRNA-Expressionsdaten log2-transformiert. *P*-Werte beziehen sich auf Log-Rank- beziehungsweise Wald-Tests. P-Werte unter 0,05 wurden als statistisch signifikant eingestuft.

1.4 Ergebnisse

TNFRSF9-Methylierung korreliert invers mit mRNA-Expression

Elf CpG-Stellen (Sonden 1-11) befinden sich in der Promotorregion (Sonden 1-5 in der Promotorregion, Sonden 6-11 in der Promotorflanke) und eine im Genkörper (Sonde 12).

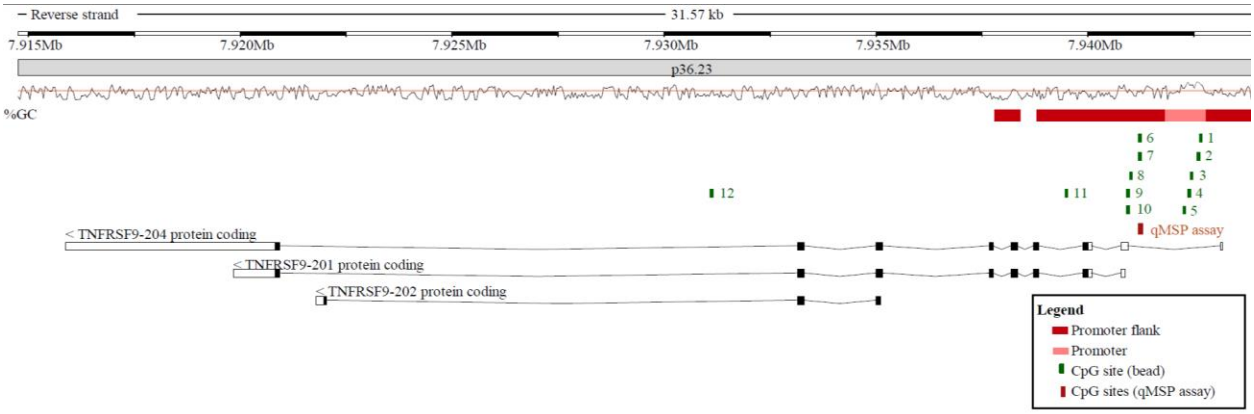

Abb. 2: Aufbau des *TNFRSF9* Gens und untersuchte CpG-Positionen. Abgebildet sind regulatorische Elemente, CG-Dichte und die Lage der HumanMethylation450 BeadChip Sonden sowie die Zielstelle des quantitativen methylierungsspezifischen PCR Assays (qMSP-Assay). Die Abbildung (modifiziert) ist aus Fröhlich und Loick et al. (2020) entnommen.

Die Korrelation zwischen der Methylierung der zwölf untersuchten CpG-Stellen und der mRNA-Expression in *N* = 468 Malignen Melanomen aus dem TCGA Research Network ergab an sechs CpGs eine signifikante inverse Korrelation. Diese war am stärksten ausgeprägt in den Promotorflanken-CpGs (Sonde 6: Spearman ρ = -0,47, *P* = <0,001; Sonde 7: ρ = -0,32, *P* = <0,001), sowie im Genkörper-CpG (Sonde 12: ρ = -0,43, *P* = <0,001). Die Methylierung der CpGs innerhalb des Promotors (Sonden 1-5) zeigte hingegen keine signifikante Korrelation mit der mRNA-Expression.

Um unsere Analysen zu detaillieren, berechneten wir die Korrelationen der *TNFRSF9*-Methylierung mit der *TNFRSF9*-mRNA-Expression des Melanomgewebes abhängig vom Ursprung des Tumorgewebes (Lymphknotenmetastase, Primärtumor, Hautmetastase, Fernmetastase) und fanden signifikant unterschiedliche *TNFRSF9*-mRNA-Expressionsniveaus. Inverse Korrelationen zwischen *TNFRSF9*-Methylierung und mRNA-Expression sind im primären Tumorgewebe, (sub-)kutanen und Fernmetastasen ausgeprägter als in Lymphknotenmetastasen. Regionale Lymphknotenmetastasen

zeigten eine höhere mRNA-Expression als Gewebe aus Primärtumoren, Haut- oder Fernmetastasen. Signifikante Unterschiede in den *TNFRSF9*-Methylierungsniveaus waren an acht von zwölf CpG-Stellen auszumachen (Positionen 1, 5, 8, 10, 12).

TNFRSF9-Methylierung korreliert mit Immunzellinfiltraten

TNFRSF9 ist ein immunstimulierendes Gen. Folglich ist davon auszugehen, dass seine Expression zur Aktivitätssteigerung tumorinfiltrierender Immunzellen führen könnte. Um diese Annahme zu bestätigen, berechneten wir Korrelationen zwischen *TNFRSF9*-mRNA-Spiegeln und der Methylierung mit dem Lymphozytenscore, der Leukozytenfraktion und den RNA-Seq-Signaturen tumorinfiltrierender Immunzellentitäten. Die wichtigsten Ergebnisse illustriert Tabelle 1.

Tab. 1: Korrelation von *TNFRSF9*-Methylierung und mRNA Expression mit dem Lymphozytenscore, der Leukozytenfraktion und dem Tumorzellgehalt. *Spearman's* Rangkorrelationskoeffizienten und P-Werte von *TNFRSF9*-Methylierung und mRNA Expression mit der Leukozytenfraktion (Saltz et al. 2018; mRNA: *N* = 468, Methylierung: *N* = 470), dem Lymphozytenscore (alle Gewebetypen; mRNA: *N* = 328, Methylierung: *N* = 329) und dem Tumorzellgehalt (% der Tumorzellnuklei; mRNA: *N* = 328, Methylierung: *N* = 329) im Malignen Melanom.

		Leukozytenfraktion		Lymphozytenscore		Tumorzellgehalt	
	CpG Stelle	*Spearman's ρ*	*P*-Wert	*Spearman's ρ*	*P*-Wert	*Spearman's ρ*	*P*-Wert
mRNA		**0.746**	**<0.001**	**0.51**	**<0.001**	**-0.134**	**0.015**
cg16839093	1	-0.026	0.58	0.08	0.13	-0.002	0.98
cg27305704	2	-0.065	0.16	-0.07	0.21	0.056	0.31
cg18859763	3	-0.065	0.16	-0.02	0.67	0.002	0.97
cg07836592	4	-0.046	0.32	-0.03	0.58	0.091	0.099
cg23959705	5	0.065	0.16	**0.14**	**0.012**	-0.003	0.96
cg06956444	6	**-0.392**	**<0.001**	**-0.31**	**<0.001**	0.038	0.50
cg14614416	7	**-0.250**	**<0.001**	**-0.22**	**<0.001**	0.029	0.60
cg18025409	8	**-0.105**	**0.023**	-0.04	0.44	0.048	0.39
cg14153654	9	**0.108**	**0.019**	0.07	0.20	**-0.126**	**0.023**
cg08840010	10	**-0.398**	**<0.001**	**-0.23**	**<0.001**	0.067	0.23
cg17123655	11	**-0.237**	**<0.001**	**-0.18**	**0.001**	0.014	0.81
cg16117781	12	**-0.484**	**<0.001**	**-0.23**	**<0.001**	0.058	0.29

Wie erwartet fanden wir eine signifikante Korrelation zwischen der TNFRSF9-mRNA-Expression mit dem Lymphozytenscore und der Leukozytenfraktion innerhalb der analysierten Immunzellen. Dabei finden sich signifikant inverse Korrelationen zwischen der *TNFRSF9*-Methylierung und dem Lymphozytenscore im Genkörper (Sonde 12) und der Promotorflankenregionen (Sonden 6, 7, 10, 11). Darüber hinaus zeigen sich signifikant inverse Korrelationen zwischen der CpG-Methylierung mit der Leukozytenfraktion in mehreren Regionen der Promotorflanke und dem Genkörper (Sonden 6 - 12). In Übereinstimmung mit der beobachteten positiven Korrelation zwischen der TNFRSF9-mRNA-Expression und der Leukozytenfraktion zeigte der Tumorzellgehalt eine signifikante negative Korrelation mit der TNFRSF9-mRNA-Expression.

Um unsere Ergebnisse der TCGA-Daten unabhängig zu bestätigen, haben wir eine Validierungskohorte mit N = 115 Melanomproben (UKB Validierungskohorte) zusammengestellt. Wir entwickelten einen methylierungsspezifischen qPCR-Test, der auf die CpG-Stelle 6 abzielt (Promotorflankenregion). Hier hatten sich in der TCGA-Kohorte stark signifikante Korrelationen zwischen Methylierung und Lymphozytenscore gezeigt. Der mittlere Lymphozytenscore betrug in der UKB Validierungskohorte 1,2 [95% CI, 0,9–1,4], der mittlere Leukozytenanteil im Tumor 5,8% [95% CI, 4,6–7,0%] und der mittlere Prozentsatz der Tumorzellen 93,7% [95% CI, 92,4 –95,0%]. Wir beobachteten signifikante inverse Korrelationen zwischen der Methylierung der CpG-Stelle 6 mit dem Lymphozytenscore (ρ = –0,24, P = 0,010) und dem Leukozytenanteil (ρ = –0,25, P = 0,008). Zusätzlich konnten wir in unserer Validierungskohorte eine positive Korrelation zwischen der Methylierung der CpG-Stelle 6 und dem Tumorzellgehalt (ρ = 0,28, P = 0,003) ausmachen. Somit konnten wir die Ergebnisse aus der TCGA-Kohorte erfolgreich validieren.

<u>Signifikante Unterschiede der *TNFRSF9*-Methylierung zwischen den Leukozytensubtypen</u>

Die stärkste inverse Korrelation zwischen Methylierung und Tumorleukozytenfraktion wurde an der CpG-Stelle 12 gefunden (Spearman ρ = –0,48, P <0,001). Daher erwarteten wir hier signifikante Methylierungsunterschiede zwischen Melanom- und Immunzellen und

möglicherweise zwischen Immunzellsubtypen. Um unsere Hypothese zu testen, analysierten wir Melanomzelllinien, primäre Melanozytenzelllinien und isolierte Leukozyten aus peripherem Blut gesunder Spender. Wir konnten signifikante Unterschiede der Methylierung zwischen allen analysierten Leukozyten (PBMCs, Monozyten, B-Zellen, $CD4^+$ - und $CD8^+$-T-Zellen), sowie Melanomzelllinien und Melanozyten bestätigen. Wie erwartet zeigten Melanomzelllinien ein hohes Maß an *TNFRFS9*-Methylierung an CpG-Stelle 12.

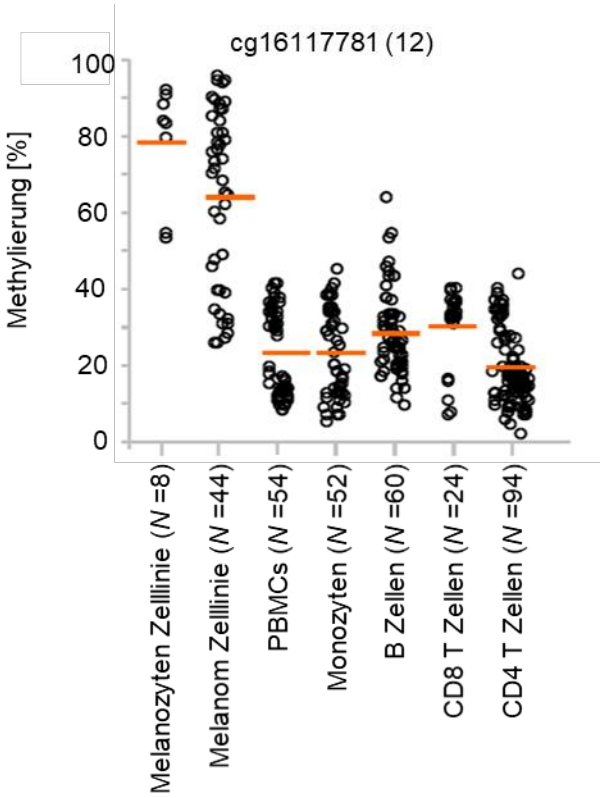

Abb. 3: *TNFRSF9* Methylierung in verschiedene Zelltypen. *TNFRSF9* Methylierung an CpG-Position 12 in Melanozyten- und Melanomzelllinien, isolierten PBMCs, Monozyten, B-Zellen, $CD8^+$ T-Zellen und $CD4^+$ T-Zellen gesunder Spender. Die Abbildung (modifiziert) ist aus Fröhlich und Loick et al. (2020) entnommen.

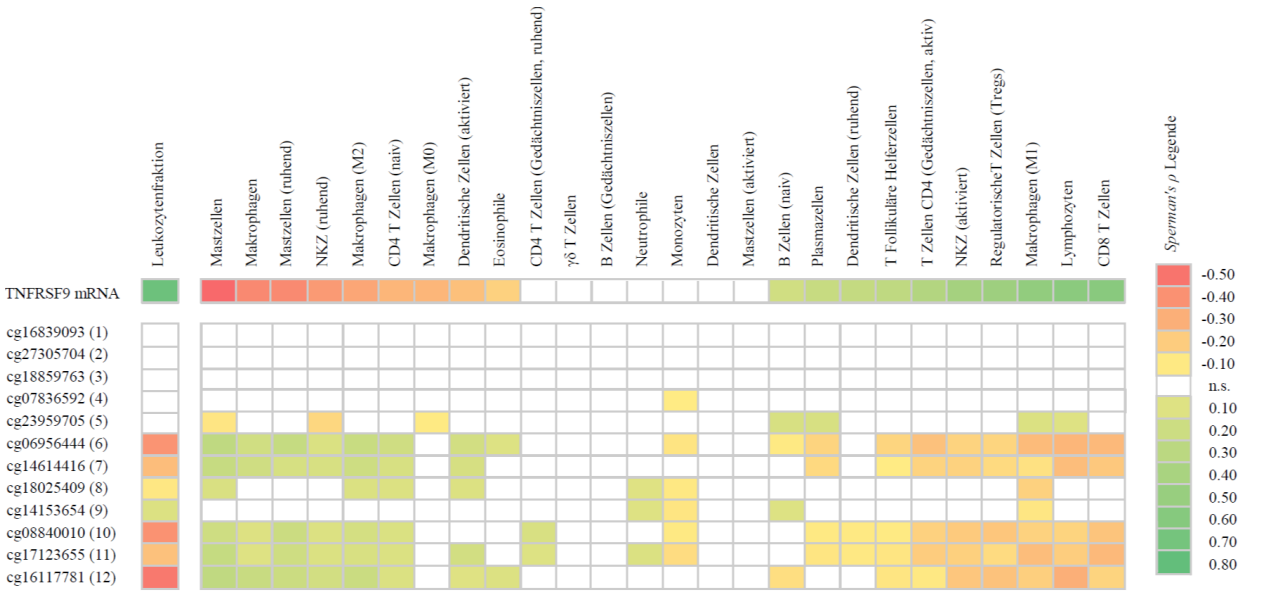

Abb. 4: Korrelationen der *TNFRSF9* Methylierung und mRNA Expression mit Immunzellinfiltraten in Melanomen. Abgebildet sind signifikante Spearman Korrelationen (*P*<0.05) zwischen *TNFRSF9*-Methylierung und mRNA-Expression mit der Leukozytenfraktion (mRNA: *N* = 468; Methylierung: *N* = 470) sowie TILs, einschließlich Lymphozyten. Die Abbildung (modifiziert) ist aus Fröhlich und Loick et al. (2020) entnommen. n.s.: nicht signifikant

TNFRSF9-Methylierung korreliert invers mit einer Interferon-γ-Signatur

Es ist bekannt, dass die TNFRSF9-Signalkaskade die Sekretion von IFNγ und die Aktivierung von $CD8^+$T-Zellen fördert (Chester, et al., 2018). Wir korrelierten daher die *TNFRSF9*-Methylierung und die mRNA-Expressionsniveaus mit der IFNγ-Signatur. Letztere haben wir durch die Expression von IFNγ- und IFNγ-regulierten Genen (*STAT1*, *STAT2*, *JAK2* und *IRF9*) definiert. *TNFRSF9*-mRNA-Expressionsniveaus korrelierten dabei positiv mit der IFNγ-Signatur. Übereinstimmend war eine inverse Korrelation der *TNFRSF9*-Methylierung (vorwiegend in der Promotorflanke und im Genkörper) mit der IFNγ-Signatur zu beobachten.

TNFRSF9-Methylierung und mRNA-Expression ist mit dem Alter assoziiert

Wir haben eine detaillierte Analyse der Assoziationen von *TNFRSF9*-Methylierung und *TNFRSF9*-mRNA-Expression mit verschiedenen klinisch-pathologischen Parametern

(u.a. TNM-Status, Gradierung, vertikale Tumordicke, Alter und Geschlecht) durchgeführt. Ausschließlich beim Alter fanden wir signifikante positive Korrelationen mit der *TNFRSF9*-Methylierung bei vier der zwölf analysierten Loci (Sonden 1, 6, 8, 11).

TNFRSF9-Methylierung und mRNA-Expression ist mit genomischen Aberrationen verbunden

Wir führten Korrelationsanalysen zwischen der *TNFRSF9*-Methylierung und mRNA-Expression mit genomischen Veränderungen durch. Signifikante Korrelationen fielen dabei zwischen der CpG-Methylierung im Promotorbereich (Sonden 1-5) und der Anzahl der Gesamtmutationen auf. Insbesondere fanden wir eine signifikante Korrelation zwischen der Methylierung von CpG-Stellen im Promotor mit Mutationen in *ARID2* (AT-reiches interaktives domänenhaltiges Protein 2; Sonden 1-5) und *IDH1* (Isocitratdehydrogenase 1; Sonden 2, 3, 5). Außerdem fanden wir signifikante Korrelationen zwischen der *TNFRSF9*-Methylierung und dem *BRAF*-Mutationsstatus an fünf der untersuchten CpG-Stellen (Sonden 5, 8, 10-12). Die *TNFRSF9*-mRNA-Expression korreliert signifikant mit der UV-Signatur (gemessen mittels C>T-Transition bei Dipyrimidinen).

TNFRSF9-Methylierung und mRNA-Expression ist mit dem Überleben assoziiert

Zur Untersuchung des Zusammenhangs zwischen der *TNFRSF9*-Methylierung und der mRNA-Expression mit dem Überleben der Patienten wurden Methylierungs- und mRNA-Expressionsniveaus als kontinuierliche log2-transformierte Variablen getestet. Die univariate Cox-Proportional-Hazards-Analyse zeigte bei Melanompatienten einen signifikanten Zusammenhang zwischen erhöhter *TNFRSF9*-mRNA-Expression und besserem Patientenüberleben (Hazard Ratio [HR] = 0,92, [95% CI: 0,87–0,97]). Übereinstimmend korrelierten erhöhte Methylierungsniveaus an sechs von zwölf CpG-Stellen signifikant mit einem schlechteren Überleben. Wir haben die mRNA-Spiegel und Methylierungswerte basierend auf optimierten Grenzwerten dichotomisiert. Kaplan-Meier-Überlebensanalysen bestätigten die bessere Prognose von Patienten mit Tumoren hoher mRNA-Expression und geringer Methylierung der CpG-Stellen in der

Promotorflankenregion und der Genkörperregion (Abb. 4 der Publikation). Überraschenderweise war eine erhöhte Methylierung von CpG-Stellen in der Promotorregion (Sonden 1, 2, 5) mit einem besseren Überleben assoziiert.

TNFRSF9-Methylierung und mRNA-Expression sind mit dem progressionsfreien Überleben unter Anti-PD-1-Immuntherapie assoziiert

Schließlich analysierten wir die *TNFRSF9*-Methylierung und die mRNA-Expression in Formalin-fixierten und Paraffin-eingebetteten Tumorgeweben im Hinblick auf das Fortschreiten der Erkrankung bei Melanompatienten, die eine Anti-PD-1-Immuntherapie erhielten. *TNFRSF9*-mRNA-Expressionsniveaus waren von *N* = 121 Anti-PD-1 behandelten Melanompatienten verfügbar, die aus einer Studie von Liu et al (mRNA-ICB-Kohorte) stammten (Liu et al., 2019). Unsere Analyse zeigte, dass kontinuierliche log2-transformierte mRNA-Spiegel signifikant mit progressionsfreiem Überleben assoziiert sind (HR = 0,92 [95 % CI: 0,85–0,99], *P* = 0,022). Dieses Ergebnis bestätigten wir mittels einer Kaplan-Meier-Überlebensanalyse nach Dichotomisierung der Methylierungswerte (optimierter Schwellenwert 1,05 TPM, Abb. 6 der Veröffentlichung).

In einer Fall-Kontroll-Studie, die *N* = 29 ansprechende und *N* = 19 nicht ansprechende, mit Anti-PD-1 behandelte Melanompatienten (UKB ICB-Kohorte) umfasst, korrelierten wir die Methylierungsniveaus mit dem progressionsfreien Überleben. Eine Signifikanz fanden wir an CpG-Stelle 12 (HR = 8,34, [95 % CI: 1,24–56,1], *P* = 0,029, Wald-Test). Wir haben dieses Ergebnis in der Kaplan-Meier-Überlebensanalyse bestätigt (optimierter Schwellenwert bei 75 % Methylierung, Abb. 5).

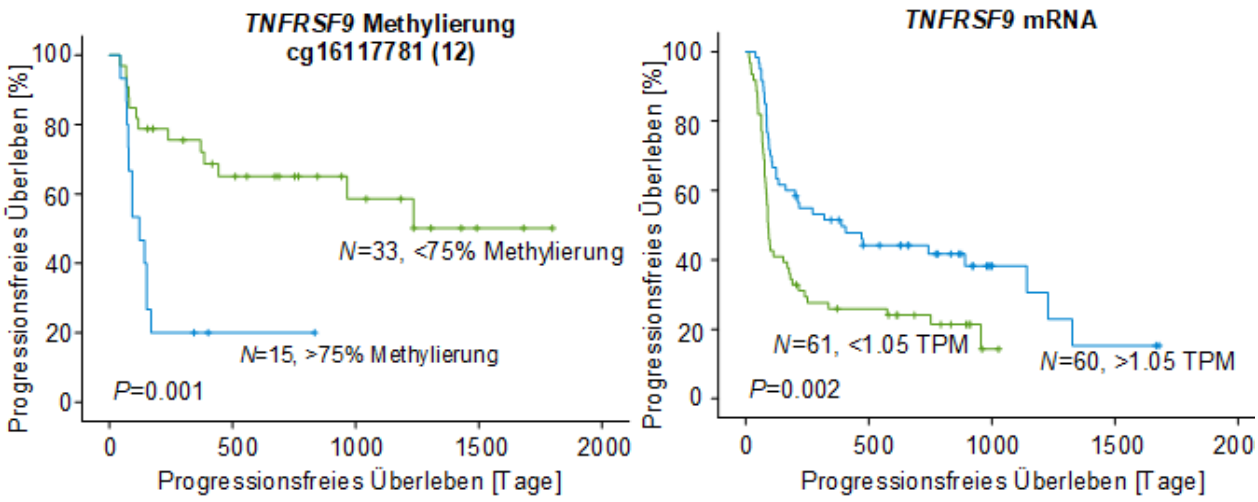

Abb. 5: Kaplan-Meier-Analyse des progressionsfreien Überlebens (PFS). Kaplan-Meier-Analyse des PFS in zwei Kohorten Anti-PD-1 behandelter Melanompatienten, dichotomisiert nach *TNFRSF9*-Methylierung an Position 12 (cg16117781) und mRNA-Expression. Die Methylierung von Position 12 wurde in einer Fall-Kontroll-Studie untersucht (UKB ICB Kohorte). Die *TNFRSF9*-mRNA-Expression wurde in *N* = 121 Proben einer Patientenkohorte ermittelt, die eine Anti-PD-1-gerichtete Immuntherapie erhielten (mRNA ICB Kohorte). Patientenproben wurden basierend auf optimierten Schwellenwerten dichotomisiert. Die Abbildung (modifiziert) ist aus Fröhlich und Loick et al. (2020) entnommen.

1.5 Diskussion

Wir untersuchten in unserer Studie einen möglichen Zusammenhang der *TNFRSF9*-DNA-Methylierung im Malignen Melanom mit der mRNA-Expression, klinisch-pathologischen, molekularen und Immunparametern und dem progressionsfreien Überleben von Melanompatienten unter Immuncheckpoint-Blockade.

Dank der Entwicklung kostengünstiger, sowie schneller Genotypisierungsmethoden wie der Illumina Infinium HumanMethylation450 konnten in den letzten Jahren in großen Mengen Daten generiert werden. Auf deren Grundlage entstanden zahlreiche Studien, die beispielsweise eine aberrante DNA-Methylierung mit dem Auftreten und Fortschreiten maligner Tumore, so auch im Melanom in Verbindung bringt (Guo et al., 2019; Micevic et al., 2017; Zhou et al., 2018).

TNFRSF9 wird auf T-Zellen und Antigenpräsentierenden Zellen (APC) exprimiert und besitzt die Fähigkeit, die Effektor-Funktionen aktivierter T-Lymphozyten zu erhöhen, die Zytokinproduktion zu steigern und die Expansion von TILs zu fördern (Bartkowiak und Curran, 2015). Palazón et al. (2012) haben in einer Mausstudie herausgefunden, dass die TNFRSF9-Expression des Tumorendothels durch Hypoxie, über den Faktor 1-alpha (HIF1-α), induziert wird. HIF1-α führt zur TNFRSF9-Hochregulation in TILs und auf diese Weise zu einer verstärkten Antitumorreaktion. Die Stimulation von TNFRSF9 vermittelt die Leukozytenextravasation, was wiederum zu einer verstärkten Migration von TILs in malignes Gewebe führt (Palazon et al., 2011). Da die TNFRSF9-Expression auf T-Zellen aktivierungsabhängig ist, ermöglicht dies bei gesunden Spendern die Identifizierung und Isolierung einer kleinen Anzahl von Antigen-spezifischen $CD8^+$T-Zellen (Wolfl et al., 2007). Weitere Studien zeigten, dass TNFRSF9 exprimierende TILs eine tumorerfahrene T-Zelllinie darstellen. Dies führt zu der Schlussfolgerung, dass die TNFRSF9-Expression zur Identifizierung von Tumorantigen-erfahrenen T-Zellen verwendet werden könnte. Dies liefert eine Grundlage für eine zelluläre Immuntherapie (Choi et al., 2014; Melero et al., 1998).

Unsere Korrelationsanalysen mit den Leukozytensubtypen stimmen mit der Funktion TNFRSF9 als kostimulierender Rezeptor überein. Es zeigen sich eine signifikante Korrelation zwischen der *TNFRSF9*-mRNA-Expression und der Infiltrationssignatur aktivierter $CD4^+$-Gedächtniszellen sowie eine negative Korrelation mit einer Signatur naiver $CD4^+$T-Zellen. Folgerichtig korreliert die *TNFRSF9*-Methylierung positiv mit der Signatur naiver $CD4^+$T-Zellen, jedoch negativ mit der Signatur aktivierter Gedächtniszellen. Ein vergleichbares Muster lässt sich auch für NK-Zellen und Makrophagen verschiedener Stadien nachweisen. Kurzgefasst heißt das, dass die *TNFRSF9*-mRNA-Expression mit Infiltrationssignaturen der aktivierten und proinflammatorischen Leukozyten korreliert, während inverse Korrelationen für ruhende NK-Zellen und entzündungshemmende Makrophagen vorliegen.

TNFRFS9-Signale fördern die Proliferation und das Überleben von regulatorischen T-Zellen (So et al., 2008). Im Gegensatz dazu wird eine negative funktionelle Rolle der TNFRSF9-Signalübertragung bei der Entwicklung dendritischer Zellen vermutet (Lee et al., 2008). Unsere Daten spiegeln diese vielseitigen Regulatorfunktionen wider: es zeigt

sich eine signifikante Korrelation zwischen der *TNFRSF9*-mRNA-Expression und den Infiltraten von Immunzellen, die mit der Verbesserung der Lymphozytenaktivierung und -infiltration bei malignen Erkrankungen assoziiert sind. Es finden sich ferner signifikante Korrelation mit der Treg-Signatur und inverse Korrelationen zwischen der *TNFRSF9*-mRNA-Expression und der Infiltrationssignatur dendritischer Zellen.

Unsere Ergebnisse deuten darauf hin, dass die *TNFRSF9*-Methylierung als Surrogat-Biomarker für TILs dienen könnte. Letztere sind mit einer besseren Prognose beim primären und fortgeschrittenen Melanom assoziiert (Azimi et al., 2012; Espinosa et al., 2017). Eine kürzlich publizierte Veröffentlichung zeigt, dass die T-Zell-Signalübertragung eine prognostische Bedeutung hat (Akbani et al., 2015). Es wurde nachgewiesen, dass die Signalübertragung im lebenden Organismus vorwiegend die $CD8^+$ T-Zellantwort beeinflusst (Vinay et al., 2006). Die Infiltration von $CD8^+$ T-Zellen ist mit einer Aktivierung der IFNγ-Wege verbunden (Topalian et al., 2016; Wu et al., 2014). Wir konnten eine signifikante Korrelation der *TNFRSF9*-mRNA-Expression mit einer IFNγ-Signatur nachweisen. Entsprechend korrelierte die *TNFRSF9*-Methylierung umgekehrt mit der mRNA-Expression von IFNγ und IFNγ-regulierten Genen. Frühere Studien wiesen nach, dass TNFRSF9 hohe IFNγ-Spiegel induziert und auf diese Weise die Tumoreliminierung unterstützt (Vinay und Kwon, 2014). Eine Phase-I-Studie bei Patienten fortgeschrittener maligner Erkrankungen, zeigte eine Antitumoraktivität unter der kombinierten Gabe des TNFRSF9-Agonisten Utomilumab mit dem Anti-PD-1-Antikörper (Tolcher et al., 2017). Es wurde eine Korrelation zwischen dem klinischen Erfolg, erhöhten $CD8^+$- Gedächtniszellen und IFNγ im Blut beobachtet. Die IFNγ-Signatur korreliert mit der Immunzellinfiltration, und beide Variablen korrelieren mit dem Überleben des Patienten bei Melanomen und anderen Krebsarten (Ni und Lu, 2018). So scheint der signifikante Zusammenhang zwischen erhöhten IFNγ-Spiegeln, der Immunzellinfiltration und der TNFRSF9-Expression folgerichtig, weil TNFRSF9 in der Hauptsache auf Immunzellen exprimiert wird. Ungeklärt bleibt jedoch auch weiterhin, ob dieTNFRSF9-Expression der Ursprung oder eine Folge der Immunzellinfiltration und der proinflammatorischen Antitumorreaktion ist.

Neben der prognostischen Bedeutung der *TNFRSF9*-Methylierung zielt unsere Studie darauf ab, eine Grundlage für weitere Tests der *TNFRSF9*-Methylierung als prädiktiven

Biomarker für Patienten, die mit TNFRSF9-Agonisten behandelt wurden zu liefern. Trotz ihres Potentials als prognostische Biomarker haben die mRNA-Expression von *TNFRSF9* und IFNγ ihre Eignung als prädiktiver Biomarker für immuntherapierte Patienten bisher nur unzureichend bewiesen (Tolcher et al., 2017). Da TILs und IFNγ allgemeine Biomarker sind, könnte die Identifizierung eines spezifischen Biomarkers von gleichzeitig prognostischer und prädiktiver Bedeutung die Möglichkeiten einer individualisierten Therapie erweitern und so besonders adjuvant hilfreich sein. In einer experimentellen Studie wurden bei 37 Lymphknotenmetastasen prädiktive Biomarker für die Reaktion auf eine Immuncheckpoint-Blockade nach ex vivo-Exposition gegenüber einer Immuncheckpoint-Blockade bei reseziertem Melanom im Stadium III untersucht (Jacquelot et al., 2017). Die Ergebnisse zeigen, dass die *TNFRSF9*-Expression auf peripheren $CD8^+$ Blut-T-Zellen mit einem besseren PFS assoziiert ist, wenn sie eine adjuvante Kombinationstherapie mit Ipilimumab und Nivolumab erhielten. Bisher wurden TNFRSF9-Antikörper nur im Rahmen von Studien verabreicht, was die Verfügbarkeit von Daten erheblich einschränkt. Daher untersuchten wir als repräsentative immuntherapierte Gruppe Patienten, die eine Anti-PD-1-gerichtete Immuncheckpoint-Blockade erhielten (mRNA ICB-Kohorte). In dieser Kohorte konnten wir nachweisen, dass *TNFRSF9*-mRNA-Expressionsniveaus signifikant mit erhöhtem PFS und dem Ansprechen auf eine Anti-PD-1-Immuntherapie assoziiert sind. Darüber hinaus fanden wir eine signifikante Korrelation der Methylierung mit dem PFS und einen deutlichen Trend zu höheren Methylierungsniveaus bei nicht ansprechenden Tumoren (UKB ICB-Kohorte). Diesen Ergebnissen zufolge liegt ein prädiktiver Wert der *TNFRSF9*-Methylierung bei immuntherapierten Melanompatienten nahe. Da Mechanismen der Antitumorreaktion, einschließlich der Infiltration von Immunzellen und der IFNγ-Expression, und der Signalisierung des Immuncheckpoints miteinander verknüpft sind, ist davon auszugehen, dass die prädiktive Bedeutung der *TNFRSF9*-Methylierung auch für Patienten gilt, die mit agonistischen TNFRSF9-Antikörpern behandelt werden.

Es wurde gezeigt, dass die *TNFRSF9*-Expression stimulationsabhängig und dynamisch ist, während die DNA-Methylierung einen konstanten Biomarker darstellt. Hier könnte die Methylierungsanalyse ein zusätzliches robustes diagnostisches Instrument darstellen. Wir schlussfolgern, dass die *TNFRSF9*-Methylierung ein prognostischer und prädiktiver Biomarker ist, der die Komplexität der molekularen Tumormikroumgebung widerspiegelt.

1.6 Zusammenfassung

Die Behandlung maligner Tumoren wurde durch die Einführung von Immuncheckpoint-Inhibitoren dramatisch verbessert. Allerdings sprechen bisher nur wenige Patienten auf diese Therapie an. Für eine Verbesserung der immunonkologischen Behandlung könnten daher zum einen alternative Immuncheckpoint-Modulatoren, zum anderen prädiktive Biomarker beitragen, anhand derer ein Patientenkollektiv mit einer voraussichtliche hohen Ansprechrate vorab identifiziert werden kann. TNFRSF 9 (4-1BB) befindet sich sowohl als Ziel einer agonistischen Immuncheckpoint-Modulation in der klinischen Entwicklung als auch in der Diskussion als potenziell prognostischer Biomarker. Die DNA-Methylierung ist ein wichtiger epigenetischer Prozess, der unter anderem während der Karzinogenese und der Immunzelldifferenzierung eine relevante Rolle spielt und daher eine ideale Quelle für die Entwicklung von Biomarkern darstellt. Ziel dieser Arbeit war es, die detaillierte Analyse der DNA-Methylierung von *TNFRSF9* im Malignen Melanom bezüglich der Eignung als Biomarker im Kontext von Immuncheckpoint-Modulatoren zu überprüfen.

Wir untersuchten die DNA-Methylierung von *TNFRSF9* hinsichtlich der Zelltypspezifität (in Melanomzelllinien und isolierten Blutleukozyten), der Transkriptionsaktivität (mRNA-Expression), dem Gesamtüberleben sowie molekularen und Immunparametern (Immunzellinfiltraten, Lymphozytenscore und Leukozytenfraktion). Wir führten mit Daten der TCGA-Kohorte Korrelationsanalysen durch und validierten die Ergebnisse stichprobenartig mittels methylierungsspzifischer qPCR in einer Kohorte von Melanompatienten des UKB. Um die Eignung als prädiktiver Biomarker für das Ansprechen auf eine Immuntherapie zu testen, griffen wir auf eine mit Anti-PD-1 behandelte Patientengruppe zurück.

Wir fanden, dass *TNFRSF9*-mRNA-Expressionsniveaus und *TNFRSF9*-Methylierung invers miteinander korrelieren. Signifikante Korrelationen konnten wir ferner zwischen der *TNFRSF9*-Methylierung und der mRNA-Expression mit dem Lymphozytenscore, der Leukozytenfraktion und der Signatur tumorinfiltrierender Leukozyten ausmachen. Unsere Korrelationsanalysen mit den Leukozytensubtypen zeigen, dass die *TNFRSF9*-mRNA-Expression mit Infiltrationssignaturen aktivierter und proinflammatorischer Leukozyten, die mit der Verbesserung der Lymphozytenaktivierung und -infiltration bei malignen Erkrankungen assoziiert sind, korreliert. Inverse Korrelationen liegen für ruhende

Leukozyten und Dendritische Zellen vor. Des Weiteren konnten wir zeigen, dass die Methylierung signifikant mit dem progressionsfreien Überleben von Melanompatienten unter Anti-PD-1-Immuntherapie assoziiert war.

Die beobachteten Korrelationen zwischen der *TNFRSF9*-DNA-Methylierung, der *TNFRSF9*-mRNA-Expression und bekannten prädiktiven Merkmalen für die positive Reaktion auf eine Immuncheckpoint-Blockade legen nahe, dass die *TNFRSF9*-Methylierung als prädiktiver Biomarker für das Therapieansprechen dienen könnte. Die Ergebnisse dieser Arbeit bilden eine Grundlage für weitere Testung der *TNFRSF9*-Methylierung als prädiktiver Biomarker einer Therapie mit TNFRSF9-Agonisten.

1.7 Literaturverzeichnis der deutschen Zusammenfassung

Absher D, Li X, Waite L, Gibson A, Roberts K, Edberg J, Chatham W, Kimberly R. Genome-wide DNA methylation analysis of systemic lupus erythematosus reveals persistent hypomethylation of interferon genes and compositional changes to CD4+ T-cell populations. PLoS genetics. 2013; 9: e1003678

Akbani R, Akdemir K, Aksoy B, Albert M, Ally A, Amin S, Arachchi H, Arora A, Auman J, Ayala B and others. Genomic classification of cutaneous melanoma. Cell. 2015; 161: 1681-1696

Amankulor N, Kim Y, Arora S, Kargl J, Szulzewsky F, Hanke M, Margineantu D, Rao A, Bolouri H, Delrow J and others. Mutant IDH1 regulates the tumor-associated immune system in gliomas. Genes & development. 2017; 31: 774-786

Armitage, R. Tumor necrosis factor receptor superfamily members and their ligands. Current opinion in immunology. 1994; 6: 407-413

Azimi F, Scolyer R, Rumcheva P, Moncrieff M, Murali R, McCarthy S, Saw R, Thompson J. Tumor-infiltrating lymphocyte grade is an independent predictor of sentinel lymph node status and survival in patients with cutaneous melanoma. Journal of clinical oncology. 2012; 30: 2678-2683

Aznar M, Labiano S, Diaz-Lagares A, Molina C, Garasa S, Azpilikueta A, Etxeberria I, Sanchez-Paulete A, Korman A, Esteller M and others. CD137 (4-1BB) costimulation modifies DNA methylation in CD8+ T cell-relevant genes. Cancer Immunol Res.. 2018; 6: 69-78

Barrett T, Wilhite S, Ledoux P, Evangelista C, Kim I, Tomashevsky M, Marshall K, Phillippy K, Sherman P, Holko M and others. NCBI GEO: archive for functional genomics data sets–update. Nucleic acids research. 2012; 41: D991-D995

Bartkowiak T, Curran M. 4-1BB Agonists: multi-Potent potentiators of tumor immunity. Frontiers in oncology. 2015; 5: 117

Chen Y, Zhang J, Wang Y, Liu N, He Q, Yang X, Sun Y, Ma J. The immune molecular landscape of the B7 and TNFR immunoregulatory ligand-receptor families in head and neck cancer: a comprehensive overview and the immunotherapeutic implications. Oncoimmunology. 2017; 6: 6e1288329

Chester C, Sanmamed M, Wang J, Melero I. Immunotherapy targeting 4-1BB: mechanistic rationale, clinical results, and future strategies. Blood, The Journal of the American Society of Hematology. 2018; 131: 49-57

Choi B, Lee S, Lee M, Kim Y, Kim Y, Ryu K, Lee J, Shin S, Lee S, Suzuki S, Oh HO, Kim CH, Lee DG, Hwang SH, Yu E, Lee IO, Kwon BS. 4-1BB-based Isolation and expansion of CD8+ T cells specific for self-tumor and non-self-tumor antigens for adoptive T-cell therapy. Journal of Immunotherapy. 2014; 37: 225-236

Chu D, Bac N. An update on anti-CD137 antibodies in immunotherapies for cancer. International journal of molecular sciences. 2019; 20: 1822

Clark E, Ledbetter J. Activation of human B cells mediated through two distinct cell surface differentiation antigens, Bp35 and Bp50. Proceedings of the National Academy of Sciences. 1986; 83: 4494-4498

Croft, M. Co-stimulatory members of the TNFR family: keys to effective T-cell immunity?. Nature Reviews Immunology. 2003; 3: 609-620

Croft, M. Costimulation of T cells by OX40, 4-1BB, and CD27. Cytokine & growth factor reviews. 2003; 14: 265-273

DeBenedette M, Chu N, Pollok K, Hurtado J, Wade W, Kwon B, Watts T. Role of 4-1BB ligand in costimulation of T lymphocyte growth and its upregulation on M12 B lymphomas by cAMP. The Journal of experimental medicine. 1995; 181: 985-992

Deutsche Krebsgesellschaft, Deutsche Krebshilfe AWMF, 2019: Leitlinienprogramm Onkologie (): Diagnostik, Therapie und Nachsorge des Melanoms, Langversion 3.2.. http://www.leitlinienprogramm-onkologie.de/leitlinien/melanom/ (Zugriffsdatum: 08.05.2020)

Edgar R, Domrachev M, Lash A. Gene expression omnibus: NCBI gene expression and hybridization array data repository. Nucleic acids research. 2002; 30: 207-210

Espinosa E, Marquez-Rodas I, Soria A, Berrocal A, Manzano J, Gonzalez-Cao M, Martin-Algarra S, Group S and others. Predictive factors of response to immunotherapy - a review from the Spanish Melanoma Group (GEM). Annals of translational medicine. 2017; 5

Fröhlich A, Loick S, Bawden E, Fietz S, Dietrich J, Diekmann E, Saavedra G, Fröhlich H, Niebel D, Sirokay J, Zarbl R, Gieleng GH, Kristiansen G, Bootz F, Landsberg J, Dietrich D. Comprehensive analysis of tumor necrosis factor receptor TNFRSF9 (4-1BB) DNA methylation with regard to molecular and clinicopathological features, immune infiltrates, and response prediction to immunotherapy in melanoma. EBioMedicine. 2020; 52: 102647

Ghoneim H, Fan Y, Moustaki A, Abdelsamed H, Dash P, Dogra P, Carter R, Awad W, Neale G, Thomas P, Youngblood B. De novo epigenetic programs inhibit PD-1 blockade-mediated t cell rejuvenation. Cell. 2017; 170: 142-157

Goltz D, Gevensleben H, Dietrich J, Dietrich D. PD-L1 (CD274) promoter methylation predicts survival in colorectal cancer patients. Oncoimmunology. 2017; 6: e1257454

Goltz D, Gevensleben H, Vogt T, Dietrich J, Golletz C, Bootz F, Kristiansen G, Landsberg J, Dietrich D. CTLA4 methylation predicts response to anti-PD-1 and anti-CTLA-4 immunotherapy in melanoma patients. JCI insight. 2018; 3: e96793

Guo W, Zhu L, Zhu R, Chen Q, Wang Q, Chen J. A four-DNA methylation biomarker is a superior predictor of survival of patients with cutaneous melanoma. eLife. 2019; 8: e44310

Hoffmann M, Tribius S. HPV and Oropharyngeal Cancer in the Eighth Edition of the TNM Classification: Pitfalls in Practice. Translational oncology. 2019; 12: 1108-1112

Hurtado J, Kim S, Pollok K, Lee Z, Kwon B. Potential role of 4-1BB in T cell. J Immunol. 1995; 155: 3360-3367

Hurtado J, Kim Y, Kwon B. Signals through 4-1BB are costimulatory to previously activated splenic T cells and inhibit activation-induced cell death. The Journal of Immunology. 1997; 158: 2600-2609

Ibrahim J, Op de Beeck K, Fransen E, Croes L, Beyens M, Suls A, Vanden Berghe W, Peeters M, Van Camp G. Methylation analysis of Gasdermin E shows great promise as a biomarker for colorectal cancer. Cancer medicine. 2019; 8: 2133-2145

Jacquelot N, Roberti M, Enot D, Rusakiewicz S, Ternes N, Jegou S, Woods D, Sodre A, Hansen M, Meirow Y and others. Predictors of responses to immune checkpoint blockade in advanced melanoma. Nature communications. 2017; 8: 1-13

Jin S, Xiong W, Wu X, Yang L, Pfeifer G. The DNA methylation landscape of human melanoma. Genomics. 2015; 106: 322-330

Jones P. Functions of DNA methylation: islands, start sites, gene bodies and beyond. Nature Reviews Genetics. 2012; 13: 484-492

Jung H, Choi S, Choi J, Kwon B. Serum concentrations of soluble 4-1BB and 4-1BB ligand correlated with the disease severity in rheumatoid arthritis. Experimental & molecular medicine. 2004; 36: 13-22

Kang Y, Kim S, Shimada S, Otsuka M, Seit-Nebi A, Kwon B, Watts T, Han J. Cell surface 4-1BBL mediates sequential signaling pathways 'downstream' of TLR and is required for sustained TNF production in macrophages. Nature immunology. 2007; 8: 601-609

Labiano S, Teijeira A, Azpilikueta A, Aznar A, Bolanos E, Melero I. Abstract 639: morphological changes in mitochondria induced by CD137 (4-1BB) co-stimulation on CD8 T cells. Cancer Res. 2017; 77: 639-639

Labiano S, Teijeira A, Azpilikueta A, Aznar A, Bolanos E, Melero I. Morphological changes in mitochondria induced by CD137 (4-1BB) co-stimulation on CD8 T cells. Cancer Research. 2017; 77: 639-639

Lee H, Park S, Choi B, Kim H, Nam K, Kwon B. 4-1BB promotes the survival of CD8+ T lymphocytes by increasing expression of Bcl-xL and Bfl-1. The Journal of Immunology. 2002; 169: 4882-4888

Lee S, Park Y, So T, Kwon B, Cheroutre H, Mittler R, Croft M. Mittler R.S. Identification of regulatory functions for 4-1BB and 4-1BBL in myelopoiesis and the development of dendritic cells. Nature immunology. 2008; 9: 917-926

Lehmann U, Kreipe H. Real-time PCR-based assay for quantitative determination of methylation status. Epigenetics Protocols. 2004; 207-218

Liu D, Schilling B, Liu D, Sucker A, Livingstone E, Jerby-Amon L, Zimmer L, Gutzmer R, Satzger I, Loquai C and others. Integrative molecular and clinical modeling of clinical outcomes to PD1 blockade in patients with metastatic melanoma. Nature Medicine. 2019; 25: 1916-1927

Sluijter BJR, van den Hout M. 4-1BB-mediated expansion affords superior detection of in vivo primed effector memory CD8+ T cells from melanoma sentinel lymph nodes. Clinical immunology. 2010; 137: 221-233

Lynch D. The promise of 4-1BB (CD137)-mediated immunomodulation and the immunotherapy of cancer. Immunological reviews. 2008; 222: 277-286

Maerten P, Geboes K, De Hertogh G, Shen C, Cadot P, Bullens D, Van Assche G, Penninckx F, Rutgeerts P, Ceuppens J. Functional expression of 4-1BB (CD137) in the inflammatory tissue in Crohn's disease. Clinical Immunology. 2004; 112: 239-46

Mamrut S, Avidan N, Staun-Ram E, Ginzburg E, Truffault F, Berrih-Aknin S, Miller A. Integrative analysis of methylome and transcriptome in human blood identifies extensive sex-and immune cell-specific differentially methylated regions. Epigenetics. 2015; 10: 943-957

Maus M, Thomas A, Leonard D, Allman D, Addya K, Schlienger K, Riley J, June C. Ex vivo expansion of polyclonal and antigen-specific cytotoxic T lymphocytes by artificial APCs expressing ligands for the T-cell receptor, CD28 and 4-1BB. Nature biotechnology. 2002; 20: 143-148

Maus M, Thomas A, Leonard D, Allman D, Addya K, Schlienger K, Riley J, June C. Ex vivo expansion of polyclonal and antigen-specific cytotoxic T lymphocytes by artificial APCs expressing ligands for the T-cell receptor, CD28 and 4-1BB. Nature biotechnology. 2002; 20: 143-148

Melero I, Johnston J, Shufford W, Mittler R, Chen L. NK1.1 cells express 4-1BB (CDw137) costimulatory molecule and are required for tumor immunity elicited by Anti-4-1BB monoclonal antibodies. Cellular immunology. 1998; 190: 167–172

Micevic G, Theodosakis N, Bosenberg M. Aberrant DNA methylation in melanoma: biomarker and therapeutic opportunities. Clinical epigenetics. 2017; 9: 34

Ni L, Lu J. Interferon gamma in cancer immunotherapy. Cancer medicine. 2018; 7: 4509-4516

Palazon A, Martinez-Forero I, Teijeira A, Morales-Kastresana A, Alfaro C, Sanmamed M, Perez-Gracia J, Penuelas I, Hervas-Stubbs S, Rouzaut A, de Landázuri MO, Jure-Kunkel M, Aragonés J, Melero I. The HIF-1 α hypoxia response in tumor-infiltrating T lymphocytes induces functional CD137 (4-1BB) for immunotherapy. Cancer discovery. 2012; 2: 608-623

Palazon A, Teijeira A, Martinez-Forero I, Hervas-Stubbs S, Roncal C, Penuelas I, Dubrot J, Morales-Kastresana A, Perez-Gracia J, Ochoa M, Ochoa-Callejero L, Martínez A, Luque A, Dinchuk J, Rouzaut A, Jure-Kunkel M, Melero I. Agonist Anti-CD137 mAb act on tumor endothelial cells to enhance recruitment of activated T lymphocytes. Cancer research. 2011; 71: 801-811

Pan Y, Liu G, Zhou F, Su B, Li Y. DNA Methylation Profiles in Cancer Diagnosis and Therapeutics. Clinical and experimental medicine. 2018; 18: 1-14

Saltz J, Gupta R, Hou L, Kurc T, Singh P, Nguyen V, Samaras D, Shroyer K, Zhao T, Batiste R, van Arnam J. Spatial organization and molecular correlation of tumor-

infiltrating lymphocytes using deep learning on pathology images. Cell reports. 2018; 23: 181-193

Schadendorf, D. Immuntherapien bei soliden Tumoren: Auf dem Weg zum Standard beim Melanom. Dtsch Arztebl International. 2015; 112: 19

Scharer C, Barwick B, Youngblood B, Ahmed R, Boss J. Global DNA methylation remodeling accompanies CD8 T cell effector function. The Journal of Immunology. 2013; 191: 3419-3429

Schwarz H, Tuckwell J, Lotz M. A receptor induced by lymphocyte activation (ILA): a new member of the human nerve-growth-factor/tumor-necrosis-factor receptor family. Gene. 1993; 134: 295-298

Segal N, He A, Doi T, Levy R, Bhatia S, Pishvaian M, Cesari R, Chen Y, Davis C, Huang B, Thall AD, Gopal AK. Phase I study of single-agent utomilumab (PF-05082566), a 4-1BB/CD137 agonist, in patients with advanced cancer. Clinical Cancer Research. 2008; 24: 1816-1823

So T, Lee S, Croft M. Immune regulation and control of regulatory T cells by OX40 and 4-1BB. Cytokine & growth factor reviews. 2008; 19: 253-262

Steegenga W, Boekschoten M, Lute C, Hooiveld G, De Groot P, Morris T, Teschendorff A, Butcher L, Beck S, Müller M. Genome-wide age-related changes in DNA methylation and gene expression in human PBMCs. Age. 2014; 36: 9648

Thorsson V, Gibbs D, Brown S, Wolf D, Bortone D, Yang T, Porta-Pardo E, Gao G, Plaisier C, Eddy J and others. The immune landscape of cancer. Immunity. 2018; 48: 812-830

Tolcher A, Sznol M, Hu-Lieskovan S, Papadopoulos K, Patnaik A, Rasco D, Di Gravio D, Huang B, Gambhire D, Chen Y, Thall AD, Pathan N, Schmidt EV, Chow LQM. Phase Ib study of utomilumab (PF-05082566), a 4-1BB/CD137 agonist, in combination with pembrolizumab (MK-3475) in patients with advanced solid tumors. Clinical Cancer Research. 2017; 23: 5349-5357

Topalian S, Taube J, Anders R, Pardoll D. Mechanism-driven biomarkers to guide immune checkpoint blockade in cancer therapy. Nature Reviews Cancer. 2016; 16: 275-287

Topalian S, Taube J, Anders R, Pardoll D. Mechanism-driven biomarkers to guide immune checkpoint blockade in cancer therapy. Nature Reviews Cancer. 2016; 16: 275-287

Ventham N, Kennedy N, Adams A, Kalla R, Heath S, O'leary K, Drummond H, Wilson D, Gut I, Nimmo E, Satsangi J. Integrative epigenome-wide analysis demonstrates that DNA methylation may mediate genetic risk in inflammatory bowel disease. Nature communications. 2016; 7: 1-14

Vinay D, Cha K, Kwon B. Dual immunoregulatory pathways of 4-1BB signaling. Journal of molecular medicine. 2006; 84: 726-736

Vinay D, Kwon B. 4-1BB (CD137), an inducible costimulatory receptor, as a specific target for cancer therapy. BMB reports. 2014; 47: 122-129

Weigelin B, Bolanos E, Teijeira A, Martinez-Forero I, Labiano S, Azpilikueta A, Morales-Kastresana A, Quetglas J, Wagena E, Sanchez-Paulete A, Chen L, Friedl P, Melero I. Focusing and sustaining the antitumor CTL effector killer response by agonist anti-CD137 mAb. Proceedings of the National Academy of Sciences. 2015; 112: 7551-7556

Weisenberger D, Siegmund K, Campan M, Young J, Long T, Faasse M, Kang G, Widschwendter M, Weener D, Buchanan D, Koh H, Simms L, Barker M, Leggett B, Levine J, Kim M, French AJ, Thibodeau SN, Jass J, Haile R, Laird PW. CpG island methylator phenotype underlies sporadic microsatellite instability and is tightly associated with BRAF mutation in colorectal cancer. Nature genetics. 2006; 38: 787-793

Wolfl M, Kuball J, Ho W, Nguyen H, Manley T, Bleakley M, Greenberg P. Activation-induced expression of CD137 permits detection, isolation, and expansion of the full repertoire of CD8+ T cells responding to antigen without requiring knowledge of epitope specificities. Blood, The Journal of the American Society of Hematology. 2007; 110: 201-210.

Wu H, Chen Y, Wang Z, Zhao Q, He M, Wang Y, Wang F, Xu R. Alteration in TET1 as potential biomarker for immune checkpoint blockade in multiple cancers. Journal for immunotherapy of cancer. 2019; 7: 264

Wu X, Zhang H, Xing Q, Cui J, Li J, Li Y, Tan Y, Wang S. PD-1^{+} CD8^{+} T cells are exhausted in tumours and functional in draining lymph nodes of colorectal cancer patients. British journal of cancer. 2014; 111: 1391-1399

Ye Q, Song D, Poussin M, Yamamoto T, Best A, Li C, Coukos G, Powell D. CD137 accurately identifies and enriches for naturally occurring tumor-reactive T cells in tumor. Clinical Cancer Research. 2014; 20: 44-55

Yi M, Jiao D, Xu H, Liu Q, Zhao W, Han X, Wu K. Biomarkers for predicting efficacy of PD-1/PD-L1 inhibitors. Molecular cancer. 2018; 17: 1-14

Zerbino D, Achuthan P, Akanni W, Amode M, Barrell D, Bhai J, Billis K, Cummins C, Gall A, Giron C and others. Ensembl 2018. Nucleic acids research. 2018; 46: D754-D761

Zhou C, Ye M, Ni S, Li Q, Ye D, Li J, Shen Z, Deng H. DNA methylation biomarkers for head and neck squamous cell carcinoma. Epigenetics. 2018; 13: 398-409

Zhu H, Mi W, Luo H, Chen T, Liu S, Raman I, Zuo X, Li Q. Whole-genome transcription and DNA methylation analysis of peripheral blood mononuclear cells identified aberrant gene regulation pathways in systemic lupus erythematosus. Arthritis Res Ther. 2016; 18: 162

3. Danksagung

Die vorliegende Dissertation wurde in der Biomarker Group unter der Leitung von PD Dr. Dimo Dietrich an der Klinik und Poliklinik für Hals-Nasen-Ohren-Heilkunde des Universitätsklinikums Bonn angefertigt. Ich möchte mich bei all denen bedanken, die mich auf vielfältige Weise bei meiner Arbeit unterstützten.

An vorrangiger Stelle möchte ich Herrn PD Dr. Dimo Dietrich für die Überlassung des Themas sowie die Betreuung bei der Anfertigung der Arbeit herzlich danken. Insbesondere gilt mein Dank für die immerwährende Unterstützung, die konstruktive Kritik, die vielen förderlichen Ratschläge sowie für die stets geöffnete Tür.

Den Mitgliedern des Arbeitskreises danke ich für Ihre Hilfsbereitschaft, Freundlichkeit und die überaus angenehme Arbeitsatmosphäre. Insbesondere möchte ich hier Frau Romina Zarbl und Timo Vogt nennen.

Frau Dr. Anne Fröhlich danke ich für all ihre Arbeit, die sie in die Veröffentlichung des Papers gesteckt hat.

Frau Prof. Dr. Marieta Toma danke ich sehr für die Einweisung und Hilfe am Mikroskop.

Ich danke meinem Mann Philipp für die Hilfe im Dschungel der englischen Sprache, Bedienungshilfen bei Excel, die Betreuung unseres Sohnes und das Aufmuntern auch zu spätester Stunde im Formatierungschaos.

EBioMedicine 52 (2020) 102647

Contents lists available at ScienceDirect

EBioMedicine

journal homepage: www.elsevier.com/locate/ebiom

Research paper

Comprehensive analysis of tumor necrosis factor receptor *TNFRSF9* (*4-1BB*) DNA methylation with regard to molecular and clinicopathological features, immune infiltrates, and response prediction to immunotherapy in melanoma

Anne Fröhlich[a,1], Sophia Loick[b,1], Emma Grace Bawden[c,d,e], Simon Fietz[a,b], Jörn Dietrich[b], Eric Diekmann[b], Gonzalo Saavedra[a,b], Holger Fröhlich[f], Dennis Niebel[a], Judith Sirokay[a], Romina Zarbl[b], Gerrit H. Gielen[g], Glen Kristiansen[h], Friedrich Bootz[b], Jennifer Landsberg[a,2], Dimo Dietrich[b,2,*]

[a] *Department of Dermatology and Allergy, University Hospital Bonn, Rheinische-Friedrich-Wilhelms-Universität Bonn, Bonn, Germany*
[b] *Department of Otolaryngology, Head and Neck Surgery, University Hospital Bonn, Rheinische-Friedrich-Wilhelms-Universität Bonn, Sigmund-Freud-Str. 25, 53105 Bonn, Germany*
[c] *Unit for RNA Biology, Department of Clinical Chemistry and Clinical Pharmacology, University Hospital Bonn, Rheinische-Friedrich-Wilhelms-Universität Bonn, 53105 Bonn, Germany*
[d] *Institute of Experimental Oncology (IEO), University Hospital Bonn, Rheinische-Friedrich-Wilhelms-Universität Bonn, 53105 Bonn, Germany*
[e] *Department of Microbiology & Immunology, The University of Melbourne at the Peter Doherty Institute for Infection & Immunity, Melbourne, VIC, Australia*
[f] *Bonn-Aachen International Center for Information Technology, Rheinische-Friedrich-Wilhelms-Universität Bonn, Bonn, Germany*
[g] *Institute of Neuropathology, University Hospital Bonn, Rheinische-Friedrich-Wilhelms-Universität Bonn, Bonn, Germany*
[h] *Institute of Pathology, University Hospital Bonn, Rheinische-Friedrich-Wilhelms-Universität Bonn, Bonn, Germany*

ARTICLE INFO

Article History:
Received 13 May 2019
Revised 16 January 2020
Accepted 16 January 2020
Available online xxx

Keywords:
TNFRSF9
DNA methylation
Melanoma
Prognostic biomarker
Predictive biomarker
Immune cell infiltration
Immune checkpoint
Immunotherapy
Response prediction
4-1BB

ABSTRACT

Background: Immunotherapy, including checkpoint inhibition, has remarkably improved prognosis in advanced melanoma. Despite this success, acquired resistance is still a major challenge. The T cell costimulatory receptor TNFRSF9 (also known as 4-1BB and CD137) is a promising new target for immunotherapy and two agonistic antibodies are currently tested in clinical trials. However, little is known about epigenetic regulation of the encoding gene. In this study we investigate a possible correlation of *TNFRSF9* DNA methylation with gene expression, clinicopathological parameters, molecular and immune correlates, and response to anti-PD-1 immunotherapy to assess the validity of *TNFRSF9* methylation to serve as a biomarker.
Methods: We performed a correlation analyses of methylation at twelve CpG sites within *TNFRSF9* with regard to transcriptional activity, immune cell infiltration, mutation status, and survival in a cohort of $N = 470$ melanoma patients obtained from The Cancer Genome Atlas. Furthermore, we used quantitative methylation-specific PCR to confirm correlations in a cohort of $N = 115$ melanoma patients' samples (UHB validation cohort). Finally, we tested the ability of *TNFRSF9* methylation and expression to predict progression-free survival (PFS) and response to anti-PD-1 immunotherapy in a cohort comprised of $N = 121$ patients (mRNA transcription), (mRNA ICB cohort) and a case-control study including $N = 48$ patients (DNA methylation, UHB ICB cohort).
Findings: We found a significant inverse correlation between *TNFRSF9* DNA methylation and mRNA expression levels at six of twelve analyzed CpG sites ($P \leq 0.005$), predominately located in the promoter flank

Abbreviations: 95% CI, 95% confidence interval; ARID2, AT-rich interactive domain-containing protein 2; BRAF, V-raf murine sarcoma viral oncogene homolog B1; IDH1, Isocitrate dehydrogenase 1; CTLA4, Cytotoxic T-lymphocyte associated protein 4; CR, Complete response; FFPET, Formalin-fixed and paraffin-embedded tissue; HIF1-α, Hypoxia-inducible factor 1-alpha; IFN-γ, Interferon gamma; IL-2, Interleukin 2; IRB, Institutional Review Board; LAG3, lymphocyte activating 3; LHR, Likelihood Ratio; MYC, MYC proto-oncogene; MAPK, Mitogen-activated protein kinase; MR, Mixed response; NA, Not assessable; NAT, Normal adjacent tissue; n.c., Normalized counts; NF-kB, Nuclear factor 'kappa-light-chain-enhancer' of activated B-cells; NK cells, Natural killer cells; OS, Overall survival; PBMCs, Peripheral blood mononucleated cells; PD, Progressive disease; PD-1, Programmed cell death 1; PD-L1, Programmed cell death 1 ligand 1; PFS, Progression-free survival; PR, Partial response; qMSP, quantitative methylation-specific PCR; SKCM, Skin cutaneous melanoma; TCGA, The Cancer Genome Atlas; TILs, Tumor infiltrating lymphocytes; TALs, Tumor-associated lymphocytes; TNFRS9, Tumor necrosis factor receptor super family 9; TPM, Transcripts per million; Tregs, Regulatory T cells

* Corresponding author.
E-mail address: dimo.dietrich@gmail.com (D. Dietrich).
[1] These authors contributed equally.
[2] These authors are joint senior authors on this work.

https://doi.org/10.1016/j.ebiom.2020.102647

region. Consistent with its role as costimulatory receptor in immune cells, TNFRSF9 mRNA expression and hypomethylation positively correlated with immune cell infiltrates and an interferon-γ signature. Furthermore, elevated TNFRSF9 mRNA expression and *TNFRSF9* hypomethylation correlated with superior overall survival. In patients receiving anti-PD-1 immunotherapy (mRNA ICB cohort), we found that *TNFRSF9* hypermethylation and reduced mRNA expression correlated with poor PFS and response.

Interpretation: Our study suggests that TNFRSF9 mRNA expression is regulated via DNA methylation. The observed correlations between *TNFRSF9* DNA methylation or mRNA expression with known features of response to immune checkpoint blockage suggest *TNFRSF9* methylation could serve as a biomarker in the context of immunotherapies. Concordantly, we identified a correlation between *TNFRSF9* DNA methylation and mRNA expression with disease progression in patients under immunotherapy. Our study provides rationale for further investigating *TNFRSF9* DNA methylation as a predictive biomarker for response to immunotherapy.

Funding: AF was partly funded by the Mildred Scheel Foundation. SF received funding from the University Hospital Bonn BONFOR program (O-105.0069). DN was funded in part by DFG Cluster of Excellence Immuno-Sensation (EXC 1023). The funders had no role in study design, data collection and analysis, interpretation, decision to publish, or preparation of the manuscript; or any aspect pertinent to the study.

Research in context

Evidence before this study

The immune checkpoint TNFRSF9 (Tumor necrosis factor receptor superfamily member 9) is an attractive new target for cancer immunotherapy and currently, two agonistic antibodies are tested in clinical trials including melanoma. So far, little is known about the regulation of immune checkpoint genes, in particularly on an epigenetic level, which is fundamental for the development of more accurate mechanism-based biomarkers. Based on the results and data of a current landscape paper provided by The Cancer Genome Atlas Network and a current multicenter study on predictive biomarkers for response to anti-PD 1 therapy, we investigated the prognostic and predictive significance of *TNFRSF9* methylation in melanoma patients with and without PD-1 directed immunotherapy.

Added value of this study

Our present study suggests a high biological significance of *TNFRSF9* gene methylation and strongly indicates that *TNFRSF9* methylation plays a role in the transcriptional regulation of *TNFRSF9*. Our results demonstrate significant correlations between *TNFRSF9* hypomethylation and patients' survival, pointing to a prognostic significance of *TNFRSF9* methylation. Finally, our independent validation analysis in melanoma patients treated with anti-PD-1 immune checkpoints provides first evidence of *TNFRSF9* methylation as a potential predictive biomarker for response to immunotherapy.

Implications of all the available evidence

Our data provide rationale for further investigating *TNFRSF9* DNA methylation as a predictive biomarker in melanoma to assist the identification of patients that might benefit from agonistic TNFRSF9 therapy as well as anti-PD-1 immune checkpoint blockade or a combination therapy of the two.

1. Introduction

The tumor necrosis factor receptor superfamily member 9 (TNFRSF9), also known as 4-1BB and CD137, is an immune costimulatory receptor [1]. TNFRSF9 is expressed on activated immune cells including natural killer (NK) cells, effector T cells and antigen presenting cells, among them dendritic cells, macrophages, and B cells [2–5]. *TNFRSF9* expression is tightly controlled and has been demonstrated to be upregulated from 12 h to up to 5 days, depending on the specific T cell stimulus [6–8] with a peak expression after 24 h [9].

In mouse models, in vivo effects of TNFRSF9 signaling activation were demonstrated to include $CD8^+$ T cell activation and tumor eradication [1,10]. Induction of the TNFRSF9 signaling pathway, via receptor binding, recruits TNFR-associated factor 1 and 2, leading to activation of the transcription factor NF-kB and the mitogen-activated protein kinase (MAPK) cascade [3,11,12]. In $CD8^+$ T cells, TNFRSF9 signaling promotes activation, proliferation and production of cytokines, interleukin 2 (IL-2) and interferon gamma (IFN-γ) [13–15]. Furthermore, TNFRSF9 signaling contributes to upregulation of members of the anti-apoptotic Bcl-2 family, thus protecting against activation-induced cell death [16–19]. In regulatory T cells (Tregs), agonistic TNFRSF9 antibody treatment can lead to inhibition of immune suppressive functions, augmenting the antitumor response [20]. Yet, the influence of TNFRSF9 on Treg cells is controversial and TNFRSF9 has also been shown to maintain the suppressive capacity of Tregs [21,22]. As well as its expression on activated immune cells, TNFRSF9 is also expressed by inflamed or hypoxic endothelial cells [23] and has been detected on tumor endothelial cells [22]. Hypoxia-mediated TNFRSF9 signaling was shown to promote migration of tumor-infiltrating lymphocytes (TILs) into malignant tissue [24]. Overall, the mechanisms summarized above make TNFRSF9 an attractive target for immunotherapy and agonistic monoclonal antibodies are currently being tested in multiple clinical trials.

Preclinical evidence for the potential therapeutic relevance of TNFRSF9 in melanomas was shown in a B16.SIY model by Weigelin et al., which demonstrated that agonistic TNFRSF9 antibodies restored the function of $CD8^+$ TILs to secrete IL-2. Furthermore, combined treatment with anti-LAG3 (lymphocyte activating 3) antibodies increased the amount of $CD8^+$ effector TILs among rejuvenated exhausted TILs [25]. In another preclinical study, utomilumab, a human IgG2 agonistic antibody to TNFRSF9, demonstrated its ability to inhibit tumor growth in a human peripheral blood lymphocyte (PBL)-SCID xenograft tumor model [26]. Currently, there are several ongoing clinical trials investigating two TNFRSF9 agonists, urelumab (Bristol-Myers Squibb, NY, USA; ClinicalTrials.gov Identifiers: NCT02253992, NCT02845323, NCT02534506, NCT02451982, NCT02658981, NCT03431948, NCT02652455) and utomilumab (Pfizer, NY, USA; ClinicalTrials.gov Identifiers: NCT03258008, NCT03704298, NCT03440567, NCT03414658, NCT03318900, NCT03364348, NCT03636503, NCT03390296, NCT02554812, NCT03217747, NCT03290937, NCT02951156) in different tumor types including melanoma.

The rapidly evolving landscape of therapeutic options in advanced melanoma requires the development of companion diagnostics for patient stratification, as not all patients respond equally to a particular medication. Prognostic biomarkers might help to identify patients with localized but aggressive disease who may potentially benefit from an adjuvant treatment. Predictive biomarkers may guide the choice of the most promising therapy. Mechanism-driven biomarkers for immune checkpoint modulators include $CD8^+$ TIL density, mutational load, and immune checkpoint gene expression [27]. A current multicenter study investigated clinical, genomic and transcriptomic data of melanoma patients to discover predictive features for individual response to anti-PD1 therapy [28]. However, to facilitate the development of more accurate mechanism-based biomarkers, precise knowledge on the regulation of immune checkpoint genes, specifically on an epigenetic level, is critical.

DNA methylation is an important epigenetic regulation mechanism, playing a fundamental role in T cell differentiation and T cell exhaustion [29–31]. A multitude of studies report on aberrant methylation of inhibitory immune checkpoint genes, i.e. *PD-1, PD-L1*, PD-1 ligand 2 (*PD-L2*), and cytotoxic T-lymphocyte associated protein 4 (*CTLA4*), in various malignancies [30,32–40]. Moreover, early data suggest *CTLA4* methylation is a predictive biomarker for anti-PD-1 and anti-CTLA-4 antibodies in patients with metastatic melanoma [41].

TNFRFS9 expression has been suggested as a biomarker for TILs in ovarian cancer and melanoma [42]. A predictive significance for response to combined anti-PD-1/CTLA-4 therapy has been demonstrated experimentally for the expression of TNFRSF9 on blood and tumor $CD8^+$ T cells and $CD4^+$ T [43]. To our knowledge there is so far no study investigating *TNFRFS9* methylation as a predictive biomarker in melanoma patients treated with immune checkpoint blockade. In this work we analyzed correlates of *TNFRSF9* methylation with mRNA expression, clinicopathological parameters, and patient outcome as well as molecular and immune correlates. We investigated the prognostic and predictive significance of *TNFRSF9* methylation in melanoma patients with and without anti-PD-1 directed immunotherapy. Our results provide rationale to further investigate *TNFRSF9* methylation as a prognostic biomarker in melanoma and as a predictive biomarker for melanoma patients who may benefit from treatment with TNFRSF9 agonists.

2. Methods

2.1. Patients

2.1.1. TCGA cohort

The data we used for our analyses are partly based on datasets of The Cancer Genome Atlas Research Network (TCGA, http://cancergenome.nih.gov/). On the whole we included a total of $N = 470$ samples from the TCGA skin cutaneous melanoma (SKCM) cohort. We analyzed one sample per patient. Only data from primary solid and metastatic tumor tissue samples were extracted to our collective, whereas solid normal tissues and additional metastatic tumor tissues were excluded from our analyses. In patients providing primary solid as well as metastatic tumor tissue only primary solid tumor tissue was included. We obtained supplementary clinicopathological and molecular data (Supplemental Table 1) from a trial previously published by the TCGA Research Network [45]. Datasets containing information about sample purity and ploidy estimates calculated using the ABSOLUTE algorithm [73] were also adopted from the TCGA Research Network. The leukocyte fraction within the tumor samples was quantified by Saltz et al. and Thorsson et al. who used DNA methylation array data to identify pure leukocyte cells [46,74]. We additionally used the results provided by Thorsson et al. [46] who calculated RNASeq signatures as estimates for distinct immune cell infiltrates using the CIBERSORT algorithm [75]. Further data on infiltrating lymphocytes were again adopted from the TCGA Research Network [45]. We included data on lymphocyte distribution (0–3; 0 = no lymphocytes within the tissue, 1 = lymphocytes present involving <25% of the tissue cross sectional area, 2 = lymphocytes present in 25 to 50% of the tissue, 3 = lymphocytes present in >50% of tissue), lymphocyte density (0–3; 0 = absent, 1 = mild, 2 = moderate, 3 = severe), and a lymphocyte score (0–6, score defined as the sum of the lymphocyte distribution and density scores).

The TCGA Research Network obtained informed consent from all patients in accordance with the Helsinki Declaration of 1975.

2.1.2. Validation cohort

In the validation analysis tumor tissue samples of $N = 115$ melanoma patients of the University Bonn were included (UHB validation cohort). The cohort was composed of tissue obtained from primary melanomas, subcutaneous and cutaneous metastases, and lymph node metastases. The tumor tissue included was obtained from patients naïve to systemic antitumor treatment, including targeted therapies or immune checkpoint blockade. Our study was approved by the Institutional Review Board (IRB) of the University Hospital Bonn.

2.1.3. Anti-PD-1 treated patients

Methylation and mRNA expression was investigated in two groups of patients who received PD-1 directed immune checkpoint blockage. *TNFRSF9* methylation levels were available from a case-control study group comprised of $N = 48$ anti-PD-1-treated patients who did not respond ($N = 19$) or responded ($N = 29$) to therapy (UHB ICB cohort). The study was approved by the local IRB. TNFRSF9 mRNA levels from samples of $N = 121$ anti-PD-1-treated patients were obtained from a recently published work by Liu and co-workers [28] (mRNA ICB cohort).

2.2. Primary cell lines and isolated immune cells

Primary melanocyte ($N = 8$) and melanoma cell lines ($N = 44$) were included from the Gene Expression Omnibus (GEO) database [76,77] (GEO accessions: GSE44662 and GSE122909) [78,79].

Peripheral blood mononuclear cells (PBMCs, $N = 54$), monocytes ($N = 52$), B cells ($N = 60$), $CD8^+$ T cells ($N = 28$), and $CD4^+$ T cells ($N = 54$) isolated from peripheral blood donated by healthy individuals was obtained from four published datasets (GSE82218, GSE71245, GSE87650, GSE59250) [80–83].

2.3. mRNA expression analysis

The mRNA expression analyses are based upon data generated by the TCGA Research Network (http://cancergenome.nih.gov/) using the Illumina HiSeq 2000 RNA Sequencing Version 2 analysis (Illumina, Inc., San Diego, CA, USA). Expression data of level 3 were obtained from the TCGA webpage and were available from $N = 468$ patient samples. Normalized counts (n.c.) per genes were calculated using the SeqWare framework via the RSEM (RNA-Seq by Expectation Maximization) algorithm [84]. In addition, we included whole-transcriptome sequencing data reported as expression in transcripts per million (TPM) provided by Liu et al. [28].

2.4. DNA preparation and bisulfite conversion

DNA from formalin-fixed and paraffin-embedded tissue (FFPET) specimens (UHB validation cohort and immunotherapy case-control study (UHB ICB cohort)) was conducted after macrodissection of tumor tissues from sections mounted on glass slides. Tissue lysis and bisulfite conversion was performed using the innuCONVERT Bisulfite All-In-One Kit (Analytik Jena, Jena, Germany) according the manufacturer's instructions.

2.5. Methylation analysis

Data on gene methylation (Infinium HumanMethylation450 BeadChip, Illumina, Inc., San Diego, CA, USA) from the TCGA Research Network were available from $N = 470$ patient samples and were downloaded from the UCSC Xena browser (www.xena.ucsc.edu). Methylation levels (β-values) were calculated: Beta-value = (Intensity_Methylated)/(Intensity_Methylated + Intensity_Unmethylated + α) [85]. The constant offset α was set to 0. HumanMethylation450 BeadChip data (β-values) from isolated immune cells were downloaded from GEO database (GSE44662, GSE122909, GSE82218, GSE71245, GSE87650, GSE59250). Methylation data from the case-control study including $N = 48$ anti-PD-1 treated patients' samples was generated using the Infinium MethylationEPIC BeadChip. β-values (values between 0 and 1) were multiplied with the factor 100% in order to approximate percent methylation (0% to 100%).

TNFRSF9 promoter methylation analysis of $N = 115$ melanomas from the University Hospital Bonn (UHB validation cohort) was performed using quantitative methylation-specific real-time PCR (qMSP) technology developed by Lehmann and Kreipe [86] in order to determine the promoter methylation levels at CpG site targeted by bead 6 (forward primer: actccataatcactataatacaataa, reverse primer: gtagtgtatttttgatgtttggta, probe$_{methylated}$: 6-FAM-ccattacttaaacacaaccgata-BHQ-1, probe$_{unmethylated}$: HEX-accattacttaaacacaaccaatat-BHQ-1). All oligonucleotides were purchased from biomers.net (Ulm, Germany). The qMSP assays amplifies the target sequence on chromosome 1: 7,941,202–7,941,277 (Genome Reference Consortium Human Build 38, GRCh38.p13, http://www.ensembl.org [87], Fig. 1). PCR reactions were performed in 20 μl volumes (buffer composition as previously described [88] containing 20 ng bisulfite converted DNA (quantified *via* UV–vis spectrophotometry) and 0.4 μM each primer and 0.2 μM each probe. qMSP was carried out using a 7900HT Fast Real-Time PCR system (Applied Biosystems, Waltham, MA, USA) with the following temperature profile: 10 min at 95 °C and 40 cycles with 15 s at 95 °C, 2 s at 62 °C, and 60 s at 52 °C. We calculated percentage methylation levels using cycle treshold (CT) values obtained from probes specifically binding to bisulfite-converted methylated (CT*methylated*) and unmethylated (CT*unmethylated*) DNA, respectively (Methylation [%] = 100%/$(1 + 2^{CTmethylated - CTunmethylated})$).

2.6. Statistics

Statistical analyses were performed using SPSS, version 23.0 (SPSS Inc., Chicago, IL, USA). Analyses regarding potential correlations of characteristics were calculated using Spearman's rank correlation (Spearman's ρ). Significance levels for the Spearman's rank correlation coefficients were computed using a large sample normal theory approximation that utilizes a *t*-distribution. Mean value comparisons were performed using Wilcoxon–Mann–Whitney *U* (two groups) and Kruskal–Wallis (>2 groups) test. One-way ANOVA and post-hoc Bonferroni test were applied to perform multiple comparisons between groups. In order to reduce the influence of age-related deaths overall survival was censored after 5 years (1825 days). Kaplan–Meier method, likelihood ratios and Cox proportional hazards regression were used for the performance of survival analyses. For Kaplan–Meier analysis methylation levels and mRNA expression levels were dichotomized based on an optimized cut-off (lowest *P*-value). Cox proportional hazards analyses were performed with continuous methylation and log2-transformed mRNA expression data (mRNA expression levels of 0 n.c. were set to 0.1 and levels of 0 TPM were set to 0.01 prior to log2-transformation). *P*-values refer to log-rank and Wald tests, respectively. Two-sided *P*-values lower than 0.05 were considered statistically significant.

2.7. Role of the funding source

The funders had no role in study design, data collection and analysis, interpretation, decision to publish, or preparation of the manuscript; or any aspect pertinent to the study. DD confirms that he had full access to all the data in the study and had final responsibility for the decision to submit for publication.

3. Results

3.1. Methylation of TNFRSF9 inversely correlates with mRNA expression

The Infinium HumanMethylation450 BeadChip contains twelve beads targeting CpG sites within the *TNFRSF9* gene locus (Fig. 1). Eleven CpG sites (targeted by beads one to eleven) were located in the promoter region (beads one to five are located in the promoter,

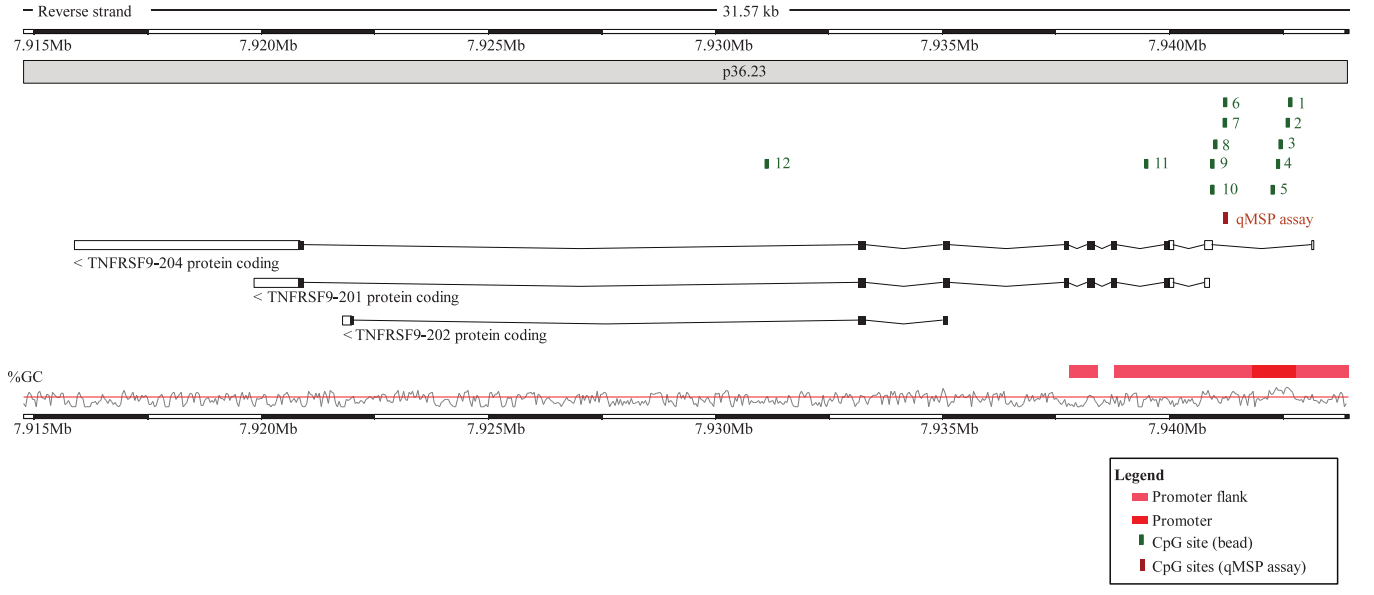

Fig. 1. Genomic organization of the *TNFRSF9* gene. Shown are regulatory elements, CG-density and target sites of HumanMethylation450 BeadChip beads and the quantitative methylation-specific PCR (qMSP assay). The modified illustration was exported from www.ensemble.org (release 98) [87] and is based on Genome Reference Consortium Human Build 38 patch release 13 (GRCh38.p13). Beads are numbered as follows: cg16839093 (1), cg27305704 (2), cg18859763 (3), cg07836592 (4), cg23959705 (5), cg06956444 (6), cg14614416 (7), cg18025409 (8), cg14153654 (9), cg08840010 (10), cg17123655 (11), cg16117781 (12).

Table 1
Correlations of *TNFRSF9* methylation with TNFRSF9 mRNA expression, lymphocyte score and overall survival. *TNFRSF9* methylation was determined at 12 different CpG sites targeted by HumanMethylation450 BeadChip beads (Fig. 1). TNFRSF9 expression was analyzed as log2-transformed variable. Significant data are shown in boldface.

		Correlation with mRNA expression[a]		Correlation with lymphocyte score[a]		Correlation with total mutations[a]		Overall survival	
Analyte	Bead no.	Spearman's ρ	*P*-value	Spearman's ρ	*P*-value	Spearman's ρ	*P*-value	Hazard Ratio [95% CI]	*P*-value
mRNA	NA	NA	NA	**0.51**	**<0.001**	0.04	0.43	**0.92 [0.87–0.97]**	**0.002**
cg16839093	1	0.06	0.23	0.08	0.13	**0.12**	**0.039**	0.20 [0.03–1.33]	0.096
cg27305704	2	0.01	0.89	−0.07	0.21	**0.15**	**0.007**	0.69 [0.31–1.53]	0.36
cg18859763	3	−0.06	0.22	−0.02	0.67	**0.12**	**0.034**	0.51 [0.15–1.76]	0.29
cg07836592	4	−0.01	0.91	−0.03	0.58	**0.13**	**0.020**	0.47 [0.15–1.53]	0.21
cg23959705	5	**0.10**	**0.025**	**0.14**	**0.012**	**0.14**	**0.013**	0.59 [0.17–2.10]	0.42
cg06956444	6	**−0.47**	**<0.001**	**−0.31**	**<0.001**	−0.01	0.91	**3.42 [1.28–9.14]**	**0.014**
cg14614416	7	**−0.32**	**<0.001**	**−0.22**	**<0.001**	−0.04	0.51	**6.28 [2.06–19.2]**	**0.001**
cg18025409	8	**−0.19**	**<0.001**	−0.04	0.44	−0.01	0.84	1.80 [0.84–3.85]	0.13
cg14153654	9	−0.02	0.62	0.07	0.20	−0.03	0.66	**3.03 [1.01–9.07]**	**0.048**
cg08840010	10	**−0.27**	**<0.001**	**−0.23**	**<0.001**	−0.03	0.57	**2.85 [1.23–6.63]**	**0.015**
cg17123655	11	**−0.32**	**<0.001**	**−0.18**	**0.001**	0.05	0.41	**3.89 [1.25–12.1]**	**0.019**
cg16117781	12	**−0.43**	**<0.001**	**−0.23**	**<0.001**	−0.04	0.52	**3.57 [1.65–7.76]**	**0.001**

NA: Not Applicable.
[a] Correlations were performed including $N = 468$ (TNFRSF9 methylation and mRNA expression), $N = 317$ (total mutations and TNFRSF9 mRNA expression), $N = 318$ (total mutations and TNFRSF9 methylation), $N = 328$ (lymphocyte score and TNFRSF9 mRNA expression), $N = 329$ (lymphocyte score and TNFRSF9 methylation) samples.

beads six to eleven in the downstream promoter flank) and one in the gene body (bead twelve).

DNA methylation in promoters is frequently associated with transcriptional gene silencing [44]. We analyzed the correlation between methylation of the twelve CpG sites and mRNA expression in $N = 468$ malignant melanoma from the TCGA Research Network [45]. We found significant inverse correlations between *TNFRSF9* DNA methylation and mRNA expression levels at six of twelve analyzed CpG sites indicating that TNFRSF9 mRNA expression may be regulated by gene methylation (Table 1). The inverse correlation was most pronounced in the promoter flank CpGs probed by bead six and seven, as well as in the gene body CpG targeted by bead twelve. Methylation of the CpGs within the promoter (targeted by beads one to five) showed no significant inverse correlation with mRNA expression.

We found significantly different TNFRSF9 mRNA expression levels among four types of tumor tissue sites (Supplemental Table 1). Regional lymph node metastases showed a higher level of mRNA expression compared to tissue obtained from primary tumors, cutaneous or distant metastases. Accordingly, significant differences in *TNFRSF9* methylation levels were found at eight of twelve CpG sites (targeted by beads one, five to eight, and ten to twelve). We further analyzed correlations of TNFRSF9 methylation with TNFRSF9 mRNA expression with regard to tumor tissue site (Supplemental Tables 1 and 2). Inverse correlations between TNFRSF9 methylation and TNFRSF9 mRNA expression in lymph nodes were similar to the general analysis including all tumor sites. However, we observed inverse correlations between TNFRSF9 methylation and mRNA expression in primary tumor tissue, distant and cutaneous/subcutaneous metastases to be more pronounced than in samples from lymph node metastases.

3.2. *Methylation of* TNFRSF9 *correlates with immune cell infiltrates*

As *TNFRSF9* is an immune stimulatory gene we predicted that its expression could augment activity of tumor infiltrating immune cells. Therefore, we investigated correlations between TNFRSF9 mRNA levels and methylation with lymphocyte score, leukocyte fraction, and RNASeq signatures of tumor infiltrating immune cell subsets. As expected, we found a significant correlation between TNFRSF9 mRNA expression with lymphocyte score and leukocyte fraction within the analyzed tumor infiltrating immune cells (Table 1, Supplemental Table 1, and Fig. 2). Accordingly, we observed significant inverse correlations between *TNFRSF9* methylation and lymphocyte score at CpG sites within the gene body and promoter flank regions probed by beads six, seven and ten to twelve (Table 1). Furthermore, there were significant inverse correlations between CpG methylation in several regions of the promoter flank and the gene body (bead target sites six to eight, ten to twelve) with the leukocyte fraction (Fig. 2). In line with the observed positive correlation between TNFRSF9 mRNA expression and leukocyte fraction, tumor cell content (percentage tumor cell nuclei in sample) showed a significant negative correlation with TNFRSF9 mRNA expression (Supplemental Table 1).

To follow up on our results based on the TCGA data we set up a validation cohort composed of $N = 115$ melanoma samples (UHB validation cohort). We designed a methylation-specific qPCR (qMSP) assay targeting CpG site six, located within the promoter flank region (Fig. 1), which had shown highly significant correlations between methylation and lymphocyte score in the TCGA cohort. In a histopathological examination we quantified leukocyte and tumor cell content as well as lymphocyte score. Mean lymphocyte score was 1.2 [95% CI, 0.9–1.4], mean percentage leukocytes in the tumor made up 5.8% [95% CI, 4.6–7.0%] and mean percentage of tumor cells were 93.7% [95% CI, 92.4–95.0%]. We observed significant inverse correlations between methylation of the CpG site six targeted by the qMSP assay and both lymphocyte score ($\rho = -0.239$, $P = 0.010$) and the leukocyte content ($\rho = -0.247$, $P = 0.008$). Accordingly, we observed a positive correlation between methylation of CpG site six with tumor cell content ($\rho = 0.279$, $P = 0.003$) in our validation cohort (UHB validation cohort).

We further performed correlative analyses stratified by tumor tissue types contained in the TCGA cohort in order to exclude the influence of sample type specific features, e.g. higher numbers of lymphocytes in lymph node metastases potentially leading to higher immune scores (Supplemental Table 3). Inverse correlations between TNFRSF9 methylation and lymphocyte score in the promoter flank regions were confirmed in four CpG sites for lymph node metastases, three CpG sites in distant metastases and two CpG sites in subcutaneous/cutaneous metastases. Methylation at CpG sites targeted by beads 6 and 10 correlated inversely with lymphocyte score for all metastatic sites. However, primary tumors showed a positive correlation between TNFRSF9 methylation and mRNA expression in the promotor region. Accordingly, a significant correlation between TNFRSF9 mRNA expression and lymphocyte score, was confirmed in the subgroup analysis for tissue obtained from lymph nodes metastases, distant metastases, and cutaneous/subcutaneous but not for primary tumors.

3.3. TNFRSF9 *methylation differs significantly between subsets of leukocytes*

The strongest inverse correlation between methylation and tumor leukocyte fraction was found at CpG site targeted by bead twelve (Spearman's $\rho = -0.484$, $P < 0.001$). Hence, we expected significant

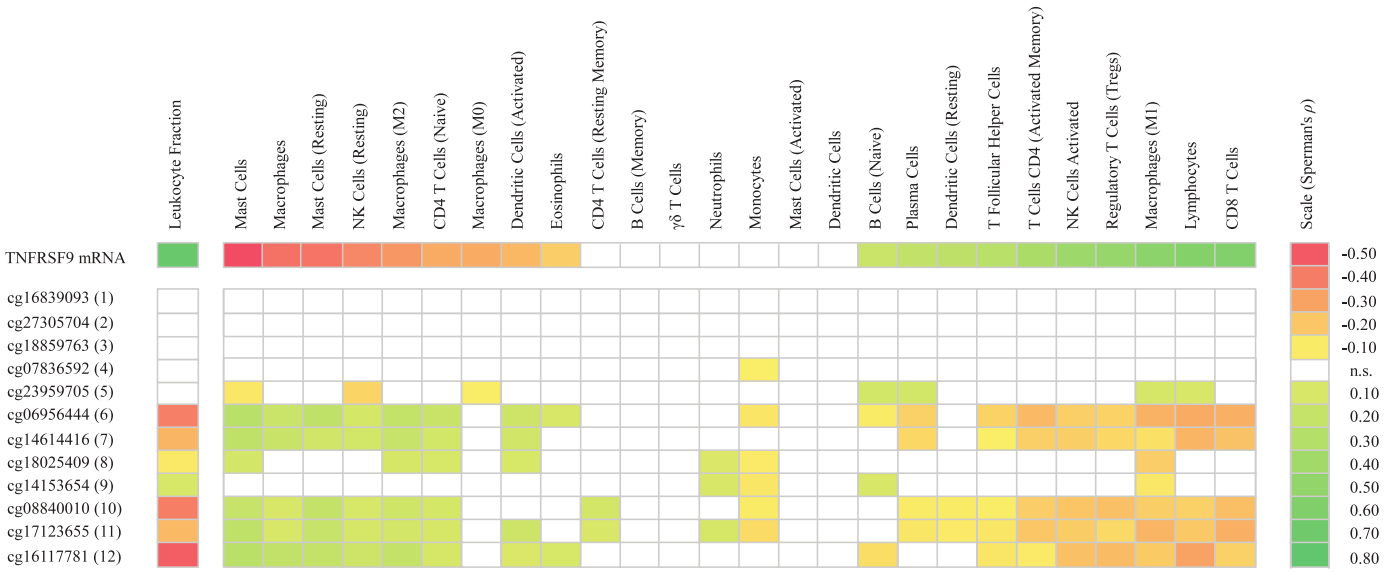

Fig. 2. Correlation of *TNFRSF9* methylation and mRNA expression with immune cell infiltrates. Shown are Spearman's ρ correlation coefficients of significance ($P<0.05$) between *TNFRSF9* methylation and mRNA expression with leukocyte fraction (mRNA: $N = 468$; methylation: $N = 470$) and distinct immune cell infiltrate signatures (mRNA: $N = 468$; methylation: $N = 469$). Immune cell infiltrates include RNA signatures of lymphocytes (including naive B cells, memory B cells, naive $CD4^+$ T cells, activated and resting $CD4^+$ memory T cells, T follicular helper cells, regulatory T cells, $CD8^+$ T cells, $\gamma\delta$ T cells, activated and resting NK cells, and plasma cells), macrophages (including monocytes and M0/M1/M2 macrophages), dendritic cells (including resting and activated dendritic cells), mast cells (including activated and resting mast cells), $CD4^+$ T cells (including naive, activated memory, and resting memory $CD4^+$ T cells), eosinophils, and neutrophils. *P*-values and Spearman's ρ correlation coefficients can be found in Supplemental Table 1; n.s.: not significant.

methylation differences between melanoma cells compared to immune cells and potentially among immune cell subtypes. In order to test our hypothesis, we analyzed primary melanoma cell lines, primary melanocyte cell lines, and isolated leukocytes from peripheral blood donated by healthy individuals. Data on the isolated leukocytes were obtained from published datasets, data for primary melanocyte and melanoma cell lines were included from the Gene Expression Omnibus (GEO) database (Fig. 3). We were able to confirm methylation differences between all analyzed leukocytes (PBMCs, monocytes, B cells, $CD4^+$ and $CD8^+$ T cells) and melanoma cell lines as well as melanocytes (Fig. 3). As expected, melanoma cell lines showed high levels of *TNFRFS9* methylation at the gene body CpG site targeted by bead 12.

We found a positive correlation between *TNFRFS9* methylation and leukocyte fraction at the promoter flank CpG site targeted by bead nine (Spearman's $\rho = 0.108$, $P = 0.019$) (Fig. 2), whereas there were no correlations with the lymphocyte score (Table 1). We therefore hypothesized there would be high methylation of total PBMCs compared to melanoma cells but no difference between melanoma cells and lymphocytes. As expected, the analysis showed no distinct differences between methylation of melanoma cells and $CD4^+$/$CD8^+$ T cells from blood of healthy donors. We did not find correlations between *TNFRFS9* methylation and leukocyte fraction in the promoter region targeted by beads one to four. Accordingly, there were no significant differences between methylation in melanoma cells and immune cells under investigation (Fig. 3). Our analysis revealed differences in *TNFRSF9* methylation within the single immune cell subtypes analyzed in the blood of healthy donors (Fig. 3).

3.4. *Methylation of* TNFRSF9 *correlates with the infiltration signature of immune cell subsets*

To gain further information concerning the composition of the immune cell infiltrates of the tumor samples contained in the TCGA cohort we used RNA signatures of tumor infiltrating leukocyte subgroups which we obtained from a study published by Thorsson et al. [46] (Fig. 2). The detailed analysis of the RNA signatures of infiltrating leukocyte subgroups revealed an infiltration signature of $CD8^+$ T cells, activated NK cells, activated $CD4^+$ T memory cells, proinflammatory M1 macrophages, Tregs and resting dendritic cells positively correlated with TNFRSF9 mRNA expression. In contrast we found an inverse correlation of infiltration signatures of resting NK cells, naïve $CD4^+$ T cells and anti-inflammatory M2 macrophages with TNFRSF9 mRNA expression (Fig. 2). Similarly, correlations between *TNFRSF9* methylation, in the promoter flank and gene body regions, and RNA-Seq signatures of tumor infiltrating immune cells depended on differentiation, activation status and inflammatory potential of the different leukocyte subsets. Infiltration signatures in the subgroups of activated NK cells, activated $CD4^+$ memory T cells and proinflammatory M1 macrophages demonstrated inverse correlations with *TNFRSF9* methylation, whereas significant correlations between *TNFRSF9* methylation and infiltration signatures were found in the corresponding subgroups of resting, naïve or anti-inflammatory leukocytes. Furthermore, we found the infiltration signature of Tregs to be inversely correlated to *TNFRSF9* methylation (Fig. 2).

3.5. *Methylation of* TNFRSF9 *inversely correlates with an interferon-γ signature*

TNFRSF9 signaling has been shown to promote the secretion IFN-γ and the activation of $CD8^+$ T cells [3]. $CD8^+$ T cells within the tumor microenvironment are associated with the activation of IFN-γ pathways [27,47]. We therefore investigated correlations between TNFRSF9 methylation and mRNA expression levels with an IFN-γ signature defined by the expression of IFN-γ and IFN-γ–regulated genes (STAT1, STAT2, JAK2, and IRF9; Table 2). TNFRSF9 mRNA expression levels positively correlated with an IFN-γ signature. Concordantly, we observed an inverse correlation of TNFRSF9 methylation levels (predominantly in the regions of the promoter flank and in the gene body) with an IFN-γ signature (Table 2).

3.6. *Methylation of* TNFRSF9 *and mRNA expression is associated with age*

A detailed analysis of associations between *TNFRSF9* methylation and TNFRSF9 mRNA expression with clinicopathological parameters

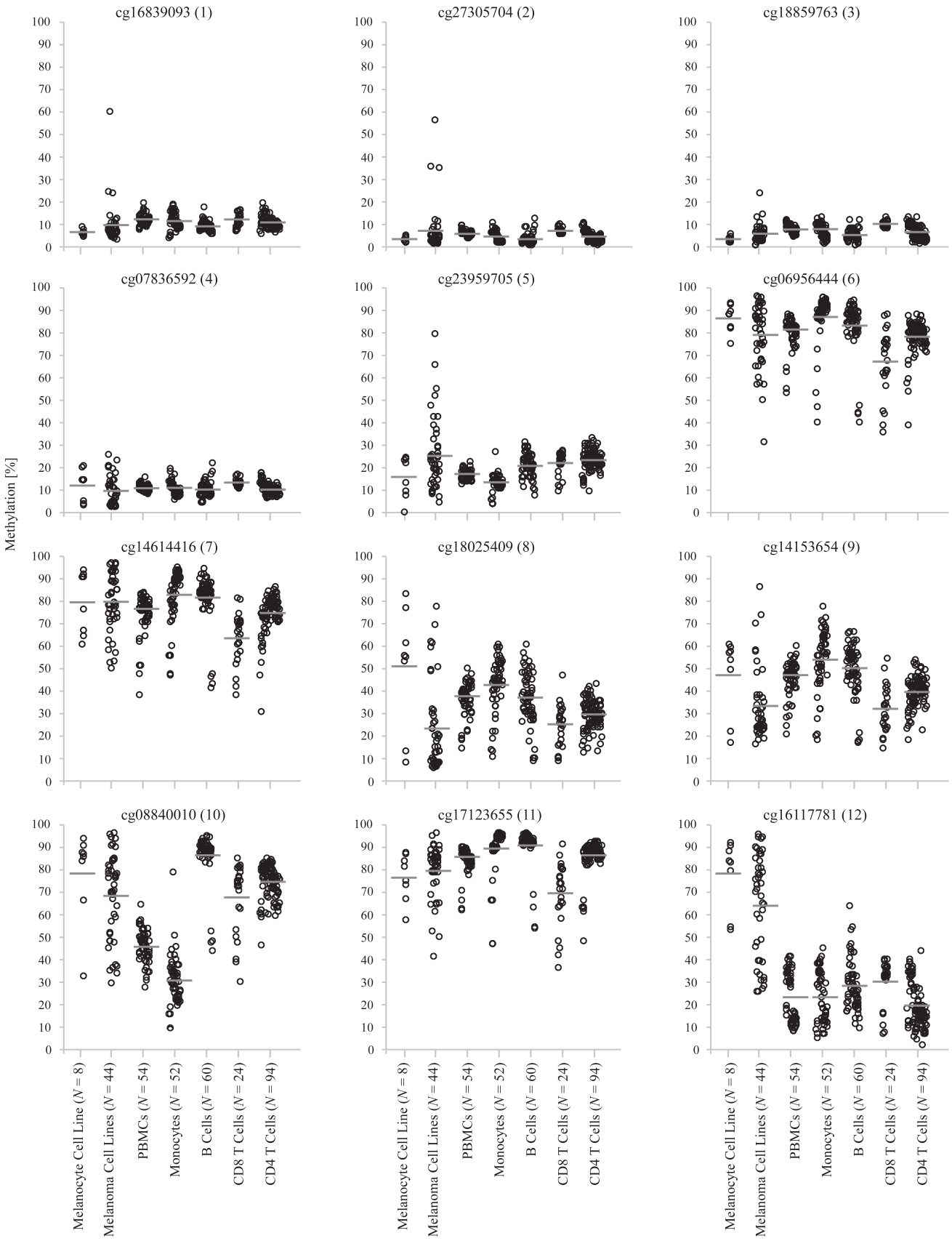

Fig. 3. *TNFRSF9* methylation in distinct cell types. *TNFRSF9* methylation at twelve CpG sites within *TNFRSF9* in primary melanoma and melanocyte cell lines as well as in isolated PBMCs, monocytes, B cells, $CD8^+$ T cells, and $CD4^+$ T cells from healthy donors. All $P < 0.001$ (Kruskal–Wallis test).

Table 2
Correlations of *TNFRSF9* methylation and mRNA expression with IFN-γ-signature. Correlations of TNFRSF9 methylation and mRNA expression with IFN-γ and IFN-γ-regulated genes (STAT1, STAT2, JAK2, and IRF9). DNA methylation was determined at twelve different loci targeted by HumanMethylation450 BeadChip beads (Fig. 1). Significant data are shown in boldface. Data were obtained from *N* = 468 (methylation) and *N* = 467 (mRNA expression) tumor samples, respectively.

		IFN-γ		STAT1		STAT2		JAK2		IRF9	
Analyte	Bead no.	Spearman's ρ	*P*-value	Spearman's ρ	*P*-value	Spearman's ρ	*P*-value	Spearman's ρ	*P*-value	Spearman's ρ	*P*-value
mRNA	NA	**0.85**	**<0.001**	**0.74**	**<0.001**	**0.31**	**<0.001**	**0.57**	**<0.001**	**0.47**	**<0.001**
cg16839093	1	0.04	0.42	0.06	0.18	0.04	0.40	**0.13**	**0.006**	0.03	0.57
cg27305704	2	0.01	0.88	0.05	0.30	0.06	0.22	**0.10**	**0.035**	0.01	0.81
cg18859763	3	−0.08	0.084	**−0.10**	**0.035**	0.00	0.98	0.02	0.61	−0.06	0.24
cg07836592	4	−0.02	0.64	−0.02	0.74	0.01	0.80	**0.10**	**0.026**	−0.02	0.62
cg23959705	5	0.07	0.15	0.09	0.064	0.05	0.27	**0.13**	**0.005**	0.08	0.082
cg06956444	6	**−0.44**	**<0.001**	**−0.40**	**<0.001**	−0.07	0.12	**−0.23**	**<0.001**	**−0.20**	**<0.001**
cg14614416	7	**−0.33**	**<0.001**	**−0.24**	**<0.001**	**−0.11**	**0.020**	**−0.14**	**0.002**	**−0.20**	**<0.001**
cg18025409	8	**−0.17**	**<0.001**	**−0.21**	**<0.001**	−0.02	0.61	**−0.10**	**0.035**	−0.09	0.051
cg14153654	9	−0.07	0.13	**−0.13**	**0.006**	−0.02	0.70	0.00	0.99	−0.05	0.24
cg08840010	10	**−0.32**	**<0.001**	**−0.31**	**<0.001**	**−0.14**	**0.002**	−0.05	0.24	**−0.27**	**<0.001**
cg17123655	11	**−0.35**	**<0.001**	**−0.36**	**<0.001**	−0.07	0.12	**−0.18**	**<0.001**	**−0.19**	**<0.001**
cg16117781	12	**−0.39**	**<0.001**	**−0.33**	**<0.001**	**−0.14**	**0.002**	**−0.24**	**<0.001**	**−0.19**	**<0.001**

NA: Not Applicable.

was performed in order to identify prognostically and biologically relevant correlates (Supplemental Table 1). We found a significant positive correlation between age and *TNFRSF9* methylation in four out of twelve analyzed loci (targeted by beads one, six, eight, and eleven). There were no relevant gender-specific differences in *TNFRSF9* methylation and mRNA expression.

3.7. *Methylation of* TNFRSF9 *and mRNA expression is associated with genomic aberrations*

We further investigated correlations between *TNFRSF9* methylation and mRNA expression with genomic alterations. Methylation of CpG sites in the promoter (targeted by beads one to five) significantly correlated with the number of total mutations. In particular, we found a significant correlation between methylation of CpG sites in the promoter with mutations in *ARID2* (AT-rich interactive domain-containing protein 2, targeted by beads one to five) and *IDH1* (Isocitrate dehydrogenase 1, targeted by beads two, three and five). Furthermore, we found a significant correlation between *TNFRSF9* methylation and *BRAF* mutation status in five CpG sites under investigation (bead target sites five, eight and ten to twelve). Regarding TNFRSF9 mRNA expression, we found significant correlations with a UV signature, indicated by C > T transitions at dipyrimidines, but no significant correlation with mutational load or *BRAF, ARID2* or *IDH1* mutation status.

3.8. *Association of* TNFRSF9 *methylation and mRNA expression with patients' survival*

Finally, we studied the association of *TNFRSF9* methylation and mRNA expression with patients' survival. Methylation and mRNA expression levels were tested as continuous log2-transformed variates without prior dichotomization in order to avoid biases due to the introduction of cutoffs for patient sample classification. In univariate Cox proportional hazards analysis, elevated TNFRSF9 mRNA expression showed a significant correlation with better patient survival (Hazard ratio [HR] = 0.92, [95% CI: 0.87−0.97], *P* = 0.002, Wald test; Table 1). Concordantly, elevated methylation levels at six out of twelve CpG sites located in the promoter flank region and the gene body region (bead target sites six, seven, and nine to twelve) were significantly correlated with poor outcome (Table 1). We further dichotomized mRNA levels and methylation levels based on optimized cut-offs for patient classification. Kaplan−Meier survival analyses confirmed the better prognosis of patients with high mRNA-expressing (above cutoff) tumors and tumors showing hypomethylation (below cutoff) of the CpG sites located in the promoter flank region and the gene body region (Fig. 4). Of note, and in contrast to the CpG sites in the promoter flank and gene body region, hypermethylation of CpG sites located in the promoter region targeted by beads one, two, and five was associated with better survival. Finally, we investigated the influence of melanoma sample type on the associations of TNFRSF9 methylation and mRNA expression with overall survival (Supplemental Table 4). We observed significant correlations of TNFRSF9 methylation and survival not only in lymph node metastases but also in distant metastases samples (Supplemental Table 4). Hence, survival differences are unlikely to be biased by the different analyzed sample types.

3.9. *Association of* TNFRSF9 *methylation and mRNA expression with anti-PD-1 response and progression-free survival*

Finally, we analyzed *TNFRSF9* methylation and mRNA expression in FFPE tumor tissues with regard to response and progression in melanoma patients who received anti-PD-1 directed immunotherapy. TNFRSF9 mRNA expression levels were available from *N* = 121 anti-PD-1 treated melanoma patients (mRNA ICB cohort) included in a study recently published by Liu et al. [28]. Our analysis demonstrated continuous log2-transformed mRNA levels to be significantly associated with progression-free survival (PFS) (HR = 0.92, [95% CI: 0.85−0.99], *P* = 0.022, Wald test). This result was confirmed in Kaplan−Meier survival analysis after result dichotomization based on an optimized cut-off (1.05 TPM, Fig. 5). Moreover, TNFRSF9 mRNA expression levels were significantly associated with response to anti-PD-1 immunotherapy (Fig. 6).

We additionally correlated continuous methylation levels with PFS in a case-control study comprised of *N* = 29 responding and *N* = 19 non-responding anti-PD-1 treated melanoma patients (UHB ICB cohort). Among the CpG sites under investigation we found methylation of CpG site targeted by bead 12 to be significantly correlated with PFS (HR = 8.34, [95% CI: 1.24−56.1], *P* = 0.029, Wald test). Again, we confirmed this result in Kaplan−Meier survival analysis after introduction of an optimized cut-off (75% methylation) for patient sample classification (Fig. 5). As expected, we also found higher mean methylation levels in samples from non-responding tumors (62.7% methylation) in comparison to samples from responding (53.4% methylation) tumors (Fig. 6), which, however, did not reach statistical significance (*P* = 0.17, Wilcoxon Mann−Whitney *U*).

4. Discussion

Epigenetic alterations, including changes in DNA methylation, have already been identified as a characteristic of T cell differentiation

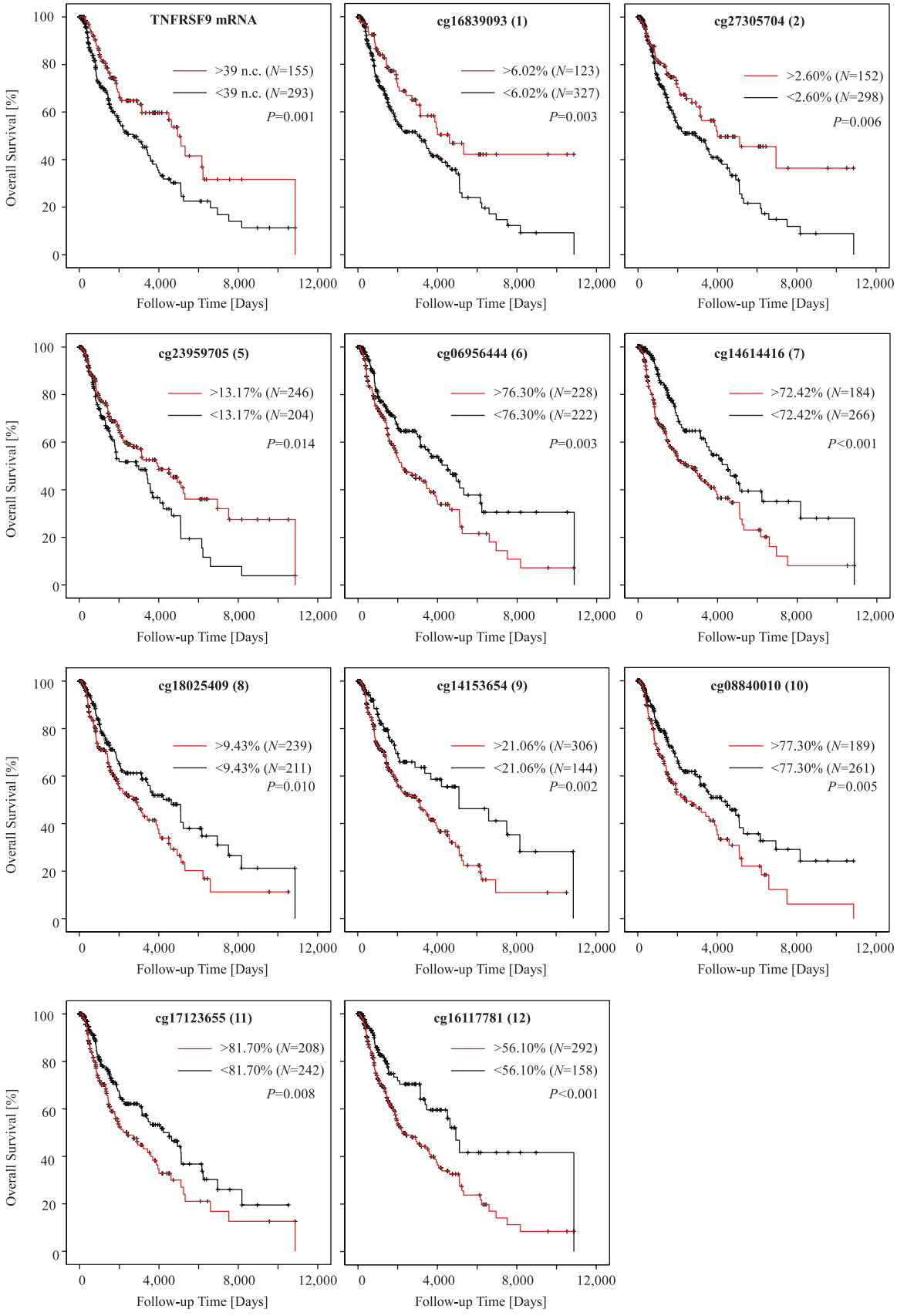

Fig. 4. Kaplan–Meier analysis of overall survival in melanoma patients stratified according to *TNFRSF9* methylation and mRNA expression. Patient samples were dichotomized based on optimized cutoffs. Analysis of CpG sites targeted by beads 3 and 4 was omitted, as generation of an optimized cutoff did not result in significant survival differences. Follow-up data was available from $N = 448$ (mRNA expression) and $N = 450$ (methylation) patients, respectively. *P*-values refer to log-rank tests.

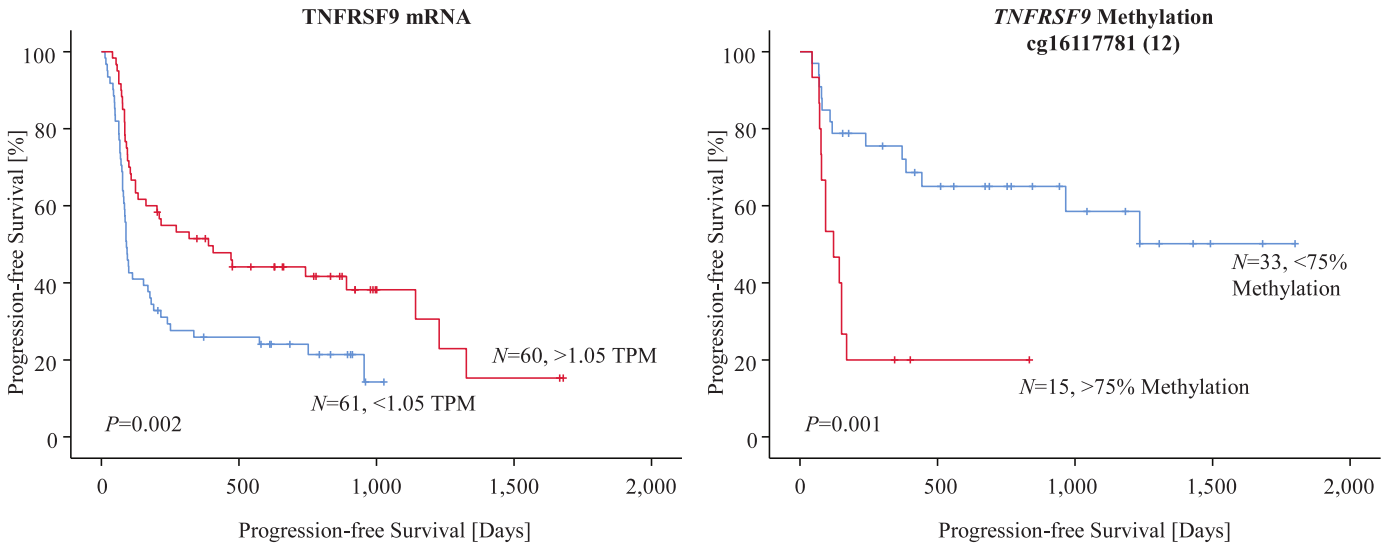

Fig. 5. Kaplan–Meier analysis of progression-free survival in two cohorts of anti-PD-1 treated melanoma patients stratified according to *TNFRSF9* methylation and mRNA expression. Methylation of CpG site targeted by bead 12 was investigated in a case-control study comprised of *N* = 19 patients with progressive disease and *N* = 29 patients with response (partial and complete), respectively, to PD-1 directed immunotherapy. TNFRSF9 mRNA expression was evaluated in *N* = 121 samples from a recently published cohort of patients who received anti-PD-1 directed immunotherapy [28]. Patient samples were dichotomized based on optimized cutoffs. *P*-values refer to log-rank tests.

[29,31,41,48,49]. Accordingly, DNA methylation is being discussed as a quantitative surrogate biomarker for T cell exhaustion [30]. Expression of the immune checkpoint CTLA-4 for example has been shown to correlate inversely with promoter methylation in diverse malignancies, supporting the use of *CTLA4* hypomethylation as a biomarker for T cell exhaustion [37,39,50] and for response to immunotherapy [41]. In our present study we investigated a possible association of *TNFRSF9* DNA methylation with mRNA expression, clinicopathological, molecular and immune parameters, survival, and response to immune checkpoint blockade in melanoma patients. The rationale behind our study was to investigate the prognostic and predictive value of *TNFRSF9* methylation in melanoma and to provide a rational for further testing *TNFRSF9* methylation as a predictive biomarker in patients treated with TNFRSF9 agonists alone or in combination with PD-1 antagonists. We observed inverse correlations between TNFRSF9 mRNA expression levels and *TNFRSF9* methylation. In addition, we found significant correlations between *TNFRSF9* methylation and mRNA expression with lymphocyte score, leukocyte fraction, and signatures of tumor infiltrating leukocytes. Our results strongly support the hypothesis that *TNFRSF9* DNA methylation regulates TNFRSF9 mRNA expression in tumor infiltrating immune cells. Finally, we showed that *TNFRSF9* DNA methylation and expressions allows for the prediction of response to anti-PD-1 targeted immunotherapy.

TNFRSF9 is expressed on both T cells and antigen presenting cells and possesses the capacity to enhance effector functions of activated T lymphocytes, to augment cytokine production and promote expansion of TILs [21]. In addition, TNFRSF9 is expressed on tumor endothelial cells and stimulation of TNFRSF9 has been shown to mediate leukocyte extravasation resulting in augmented migration of TILs into malignant tissue [22]. In a mouse study, Palazón et al. identified hypoxia to be the microenvironmental factor inducing tumor endothelial TNFRSF9 expression via hypoxia-inducible factor 1-alpha (HIF1-α). The authors also demonstrated that HIF1-α induces TNFRSF9 upregulation in TILs, resulting in an augmented antitumor response [24]. TNFRSF9 expression on T cells is activation dependent. In healthy donors, this characteristic enables identification and isolation of small numbers of antigen-specific $CD8^+$ T cells [9]. Further studies demonstrated that TILs expressing TNFRSF9 represented a tumor-experienced T cell lineage, leading to the conclusion that TNFRSF9 expression could be used to identify tumor antigen-experienced T cells, providing the rationale for adoptive T cell therapy

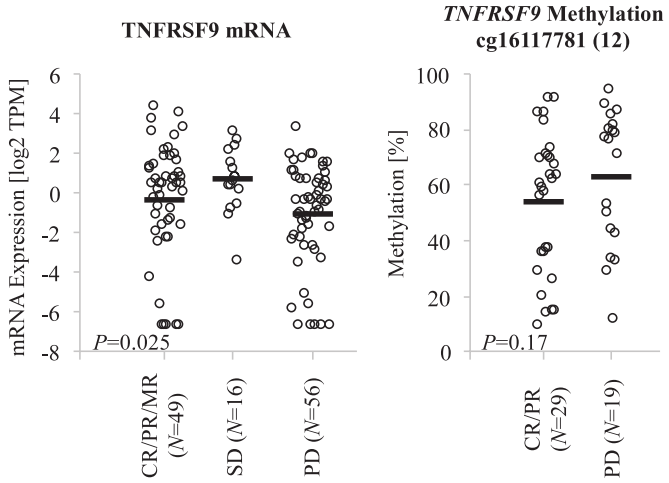

Fig. 6. *TNFRSF9* methylation and mRNA expression with regard to response to anti-PD-1 immunotherapy. TNFRSF9 mRNA expression levels in samples from a recently published anti-PD-1-treated cohort comprised of *N* = 49 responding patients (partial, mixed, and complete), *N* = 56 non-responding patients, and *N* = 16 patients with stable disease [28]. *TNFRSF9* methylation at CpG targeted by bead 12 in melanoma samples from *N* = 19 responding (complete and partial responses) and *N* = 29 non-responding patients. *P*-values refer to Wilcoxon Mann–Whitney *U* and Kruskal–Wallis test, respectively. Mean levels are indicated by bars.

[51,52]. Correspondingly, our data demonstrated a significant correlation between TNFRSF9 mRNA expression and an infiltration signature of activated $CD4^+$ memory cells and a negative correlation with a signature of naïve $CD4^+$ T cells. Conversely, *TNFRSF9* methylation correlated positively with the signature of naïve $CD4^+$ T cells but negatively with the signature of activated memory cells. We observed a similar pattern for NK cells and macrophages in different stages of activation and differentiation. That is, TNFRSF9 mRNA expression correlated with infiltration signatures of the activated and pro-inflammatory leukocyte subset, whereas inverse correlations were observed for resting NK cells and anti-inflammatory macrophages. The results are in line with the reported biological function of TNFRSF9 as a co-stimulatory receptor on activated immune cells. Furthermore, our data reflect the complex regulatory functions of TNFRSF9, as indicated by the inverse correlations of TNFRSF9 mRNA

expression with an infiltration signature of dendritic cells and the significant correlation with a signature of Tregs. TNFRFS9 signaling has been reported to promote proliferation and survival of Tregs [53]. In the development of dendritic cells however, TNFRSF9 signaling was suggested to play a negative functional role [54].

Our results demonstrate a correlation between TNFRSF9 expression and immune cell infiltrates which is consistent with the reported function of TNFRSF9 to enhance lymphocyte activation and infiltration in malignancies. In melanoma and ovarian cancer TNFRFS9 expression was suggested as a biomarker for TILs [42]. Beyond, our results indicate that methylation of *TNFRSF9* might serve as a surrogate biomarker for tumor infiltrating immune cells. Tumor infiltrating lymphocytes are known to be associated with favorable prognosis in primary and advanced melanoma [48,55]. The recent landscape paper of the TCGA cohort further suggested that T cell signaling has prognostic significance, which was in particular true for $CD8^+$ effector T cells [45]. Even though in vitro signaling of TNFRSF9 was shown to support both $CD4^+$ and $CD8^+$ T cell response, in vivo signaling was demonstrated to predominantly affect $CD8^+$ T cell response [56]. Infiltration of $CD8^+$ T cells is associated with an activation of the IFN-γ pathways [27,47]. We observed a significant correlation of TNFRSF9 mRNA expression with an IFN-γ signature. Correspondingly, TNFRSF9 methylation correlated inversely with mRNA expression of IFN-γ and IFN-γ-regulated genes. Previous studies demonstrated the ability of TNFRSF9 to induce high levels of IFN-γ, thereby improving tumor eradication [1]. A phase I trial combining the TNFRSF9 agonist, utomilumab, with anti PD-1 antibody, pembrolizumab, demonstrated antitumor activity in patients with advanced malignancies [57]. Although the study was not designed to detect relationships between clinical outcome and potential biomarkers, the authors observed a correlation between clinical benefit and elevated $CD8^+$ memory cells and IFN-γ in the peripheral blood. IFN-γ signature correlates with immune cell infiltration, and both variables are known to correlate with patient survival in melanoma and many other types of cancers [58]. As such, a correlation between elevated levels of IFN-γ, immune cell infiltration and TNFRSF9 expression seems predictable, given the fact that TNFRSF9 is predominantly expressed on immune cells. The question of causality remains; whether TNFRSF9 expression is the source or result of immune cell infiltration and proinflammatory antitumor response. An experimental study following up on the role of TNFRSF9 in the interaction between TILs and tumors cells in melanoma and ovarian cancer demonstrated that TNFRSF9 was preferentially expressed on tumor-reactive subsets of TILs and that direct contact with tumor cells stimulated the expression of TNFRSF9 [42]. These results indeed support the idea that initially TNFRSF9 expression is the result of immune cell infiltration. Based on their results the authors suggested TNFRSF9 as a biomarker for tumor-reactive TILs, assuming that TNFRSF9 expression might predict improved prognosis in ovarian cancer and melanoma. Our results support this idea.

As discussed in our study, TNFRFS9 signaling has been shown to support $CD4^+$ and $CD8^+$ T cell responses. In $CD8^+$ T cells TNFRFS9 signaling promotes cytokine production, including IFN-γ [1]. We therefore assume that TNFRFS9 expression might indicate increased cytokine levels. Ye et al. demonstrated that CD137 positive TILs and tumor-associated lymphocytes (TALs) secreted IFN-γ in response to autologous tumor cell stimulation, whereas CD137 negative TILs and TALs did not. The study showed that increased CD137 expression among $CD8^+$ TILs in the presence of tumor cells was MHC-dependent, ruling out activation-independent effects mediated by cytokines alone [42]. It has been highly documented that IFN-γ correlates with immune cell infiltration and both variables serve as generally accepted prognostic biomarkers in malignancies. Our results, in conjunction with published knowledge on TNFRFS9, support the idea to further investigate the prognostic value of TNFRSF9 expression and its epigenetic regulation.

Beyond the prognostic significance of *TNFRSF9* methylation, our study primarily aims at supplying a rational for further testing of *TNFRSF9* methylation as a predictive biomarker in a cohort of patients treated with TNFRSF9 agonists. Despite its value as prognostic biomarkers, immune checkpoint mRNA expression and IFN-γ have only insufficiently proven their suitability as predictive biomarker for patients treated with immunotherapy [59]. Whereas TILs or IFN-γ are general biomarker, the identification of a specific biomarker of concomitant prognostic and predictive significance could extend the possibilities of patient-tailored therapy and be of great value in particular in the adjuvant setting. A current trial studied predictive biomarkers for response to immune checkpoint blockade in 37 lymph node metastases after *ex vivo* exposure to immune-checkpoint blockade in resected stage III melanoma [43]. The experimental study demonstrated TNFRSF9 expression on $CD8^+$ peripheral blood T cells to be associated with progression-free survival in resected stage III melanoma patients who received adjuvant treatment with ipilimumab + nivolumab combination therapy, but not nivolumab alone. So far, agonistic TNFRSF9 antibodies have only been used in clinical trials, limiting the availability of data and samples from TNFRSF9 antibody treated patients. To investigate the feasibility of *TNFRSF9* methylation as a predictive biomarker, we therefore investigated patients who received anti-PD-1 directed immune checkpoint blockage as a representative immunotherapy study group (mRNA ICB cohort). In this group, we demonstrated TNFRSF9 mRNA expression levels to be significantly associated with increased PFS and with response to anti-PD-1 immunotherapy. Furthermore, we found methylation to be significantly correlated with PFS and a marked trend towards higher mean methylation levels in non-responding tumors in comparison to tumors responding to anti-PD-1 therapy (UHB ICB cohort). These results provide first evidence of a predictive value of *TNFRSF9* methylation in melanoma patients treated with immunotherapy. Given that mechanisms of anti-tumor response, including immune cell infiltration and IFN-γ expression, and immune checkpoint signaling are interlinked, we assume that the predictive significance of TNFRSF9 will also hold true for patients treated with agonistic TNFRSF9 antibodies. Analysis of TILs and TIL signature demands immunohistochemistry and RNAseq, with the latter being limited in FFPET. Beyond, TNFRSF9 expression has been shown to be stimulation dependent and temporally limited, whereas DNA methylation constitutes a rather robust marker. Here, methylation analysis could present an additional diagnostic tool. We therefore assume methylation of *TNFRSF9* to be a sensible prognostic and predictive biomarker reflecting the complex molecular interplay of tumor microenvironment.

A recent study demonstrated that TNFRSF9 co-stimulation in $CD8^+$ T cells leads to changes in DNA methylation and chromatin reprogramming in diverse immune-related genes [60]. In our study we investigated associations of methylation in TNFRSF9 with genomic alterations. We found a positive correlation between *TNFRSF9* promoter methylation and the presence of somatic mutations in *ARID2* and *IDH1*. Mutations in *ARID2,* encoding a component of the chromatin-remodeling complex, and the epigenetic regulator IDH1 are known to play a role in melanomagenesis [61]. The association of mutations in epigenetic enzymes and *TNFRSF9* methylation could point to a possible significance of *TNFRSF9* promoter methylation during malignant transformation. To our knowledge a tumor cell-intrinsic role of TNFRSF9 in melanoma has not been described yet and should be followed up in functional experiments.

We found significant higher levels of *TNFRSF9* methylation in *BRAF* wildtype compared to mutated melanoma. A recent study identified a network of BRAF-regulated transcription factors, including HIF1-α, that controls glycolysis in melanoma cells, is critical for response to BRAF inhibition and is modulated by BRAF inhibition in melanoma [62]. A strong link between *BRAF* mutation and DNA hypermethylation, also referred to as CpG island methylator phenotype (CIMP), has

been described in colorectal cancers [36,63]. A similar association in melanoma, however, could not be confirmed [64]. Comprehensive analyses of the data provided by TCGA identified a negative correlation between *BRAF* mutations and methylation changes in melanoma [45,46]. These results are in line with previous work demonstrating that mutations in *BRAF* [65] enhance the immune infiltrate, while those in IDH1 reduce immune cell infiltration [66]. The possibility of TNFRSF9 playing a role in the cross-talk of transcriptional regulators in melanoma needs to be followed up in future experimental studies.

We found significant correlations between age and *TNFRSF9* methylation which is in line with published studies. Age-associated methylation changes of regulatory elements have been shown to predominantly affect genes involved in immune processes [67,68], e.g. immune checkpoint genes [69,70] or genes controlling T cell immune response [71], which might serve as a possible explanation for carcinogenesis in elderly patients. A recent study revealed age-related genome-wide changes in DNA methylation in human PBMCs (peripheral blood mononucleated cells), with a functional analysis showing a strong enrichment of genes involved in cancer in older subjects [72].

In conclusion, our results suggest that TNFRSF9 mRNA expression is regulated via DNA methylation. The observed correlations between *TNFRSF9* DNA methylation, TNFRSF9 mRNA expression and known features of response to immune checkpoint blockage suggest that *TNFRSF9* methylation could be a biomarker in the context of immunotherapies. Our study provides first evidence of *TNFRSF9* as a potential predictive biomarker for response to anti-PD-1 checkpoint blockade. Based on our results, we recommend testing *TNFRSF9* DNA methylation as a predictive biomarker in patients treated with TNFRSF9 agonists and PD-1 antagonists.

Acknowledgments

We thank the BioBank Bonn of the Bonn University Medical Faculty and the University Hospital Bonn for the support of this study.

Funding source

AF was partly funded by the Mildred Scheel Foundation. SF received funding from the University Hospital Bonn BONFOR program (O-105.0069). DN was funded in part by DFG Cluster of Excellence ImmunoSensation (EXC 1023).

Disclosure statement

DD owns patents and patent applications on methylation of immune checkpoint genes (including *TNFRSF9*) as predictive and prognostic biomarkers (DE102017125780, DE102016005947, DE102015009187, WO2019086642, US2019249258, CN109715829, EP3458602, JP2019516383, WO2017198617, EP3322819, WO2017008912, CN108138242). The patents are licensed to Qiagen GmbH (Hilden, Germany) and DD receives royalties from Qiagen. DD is a consultant for AJ Innuscreen GmbH (Berlin, Germany), a 100% daughter company of Analytik Jena AG (Jena, Germany), and receives royalties from product sales (innuCONVERT kits). AF has received speaker's honoraria or travel expense reimbursements from the following companies: Novartis, BMS, Almirall, and Eli Lilly Pharma. DN has received speakers' honoraria or travel expense reimbursements from the following companies: BMS, Novartis, GSK, Celgene, and MSD. JS received speaker's honoraria from Novartis, BMS, MSD, and Roche. JL is a consultant/advisory board member of Bristol-Myers Squibb, Merck, Novartis, and Roche. No potential conflicts of interest were disclosed by the other authors.

Supplementary materials

Supplementary material associated with this article can be found in the online version at doi:10.1016/j.ebiom.2020.102647.

References

[1] Vinay DS, Kwon BS. 4-1BB (CD137), an inducible costimulatory receptor, as a specific target for cancer therapy. BMB Rep 2014;47(3):122–9.
[2] Alderson MR, Smith CA, Tough TW, Davis-Smith T, Armitage RJ, Falk B, et al. Molecular and biological characterization of human 4-1BB and its ligand. Eur J Immunol 1994;24(9):2219–27.
[3] Chester C, Sanmamed MF, Wang J, Melero I. Immunotherapy targeting 4-1BB: mechanistic rationale, clinical results, and future strategies. Blood 2018;131(1):49–57 04.
[4] Futagawa T, Akiba H, Kodama T, Takeda K, Hosoda Y, Yagita H, et al. Expression and function of 4-1BB and 4-1BB ligand on murine dendritic cells. Int Immunol 2002;14(3):275–86.
[5] Pollok KE, Kim YJ, Hurtado J, Zhou Z, Kim KK, Kwon BS. 4-1BB T-cell antigen binds to mature B cells and macrophages, and costimulates anti-mu-primed splenic B cells. Eur J Immunol 1994;24(2):367–74.
[6] Cannons JL, Lau P, Ghumman B, DeBenedette MA, Yagita H, Okumura K, et al. 4-1BB ligand induces cell division, sustains survival, and enhances effector function of CD4 and CD8 T cells with similar efficacy. J Immunol 2001;167(3):1313–24.
[7] Dawicki W, Watts TH. Expression and function of 4-1BB during CD4 versus CD8 T cell responses in vivo. Eur J Immunol 2004;34(3):743–51.
[8] Watts TH. TNF/TNFR family members in costimulation of T cell responses. Annu Rev Immunol 2005;23:23–68.
[9] Wolfl M, Kuball J, Ho WY, Nguyen H, Manley TJ, Bleakley M, et al. Activation-induced expression of CD137 permits detection, isolation, and expansion of the full repertoire of CD8+ T cells responding to antigen without requiring knowledge of epitope specificities. Blood 2007;110(1):201–10.
[10] Seo SK, Choi JH, Kim YH, Kang WJ, Park HY, Suh JH, et al. 4-1BB-mediated immunotherapy of rheumatoid arthritis. Nat Med 2004;10(10):1088–94.
[11] Sabbagh L, Pulle G, Liu Y, Tsitsikov EN, Watts TH. ERK-dependent Bim modulation downstream of the 4-1BB-TRAF1 signaling axis is a critical mediator of CD8 T cell survival in vivo. J Immunol 2008;180(12):8093–101.
[12] Vinay DS, Kwon BS. Role of 4-1BB in immune responses. Semin Immunol 1998;10(6):481–9.
[13] Lynch DH. The promise of 4-1BB (CD137)-mediated immunomodulation and the immunotherapy of cancer. Immunol Rev 2008;222:277–86.
[14] Segal NH, He AR, Doi T, Levy R, Bhatia S, Pishvaian MJ, et al. Phase I study of single-agent utomilumab (PF-05082566), a 4-1BB/CD137 Agonist, in patients with advanced cancer. Clin Cancer Res 2018;24(8):1816–23.
[15] Vinay DS, Kwon BS. Therapeutic potential of anti-CD137 (4-1BB) monoclonal antibodies. Exp Opin Ther Targets 2016;20(3):361–73.
[16] Hurtado JC, Kim YJ, Kwon BS. Signals through 4-1BB are costimulatory to previously activated splenic T cells and inhibit activation-induced cell death. J Immunol 1997;158(6):2600–9.
[17] Labiano S, Teijeira Á, Azpilikueta A, Aznar Á, Bolaños E, Melero I. Abstract 639: morphological changes in mitochondria induced by CD137 (4-1BB) co-stimulation on CD8 T cells. Cancer Res 2017;77(13 Supplement):639. –639.
[18] Maus MV, Thomas AK, Leonard DGB, Allman D, Addya K, Schlienger K, et al. Ex vivo expansion of polyclonal and antigen-specific cytotoxic T lymphocytes by artificial APCs expressing ligands for the T-cell receptor, CD28 and 4-1BB. Nat Biotechnol 2002;20(2):143–8.
[19] Takahashi C, Mittler RS, Vella AT. Cutting edge: 4-1BB is a bona fide CD8 T cell survival signal. J Immunol 1999;162(9):5037–40.
[20] Smith SE, Hoelzinger DB, Dominguez AL, Van Snick J, Lustgarten J. Signals through 4-1BB inhibit T regulatory cells by blocking IL-9 production enhancing antitumor responses. Cancer Immunol Immunother 2011;60(12):1775–87.
[21] Bartkowiak T, Curran MA. 4-1BB Agonists: multi-Potent potentiators of tumor immunity. Front Oncol 2015;5:117.
[22] Palazón A, Teijeira A, Martínez-Forero I, Hervás-Stubbs S, Roncal C, Peñuelas I, et al. Agonist Anti-CD137 mAb act on tumor endothelial cells to enhance recruitment of activated T lymphocytes. Cancer Res 2011;71(3):801–11.
[23] Teijeira Á, Palazón A, Garasa S, Marré D, Aubá C, Rogel A, et al. CD137 on inflamed lymphatic endothelial cells enhances CCL21-guided migration of dendritic cells. FASEB J 2012;26(8):3380–92.
[24] Palazón A, Martínez-Forero I, Teijeira A, Morales-Kastresana A, Alfaro C, Sanmamed MF, et al. The HIF-1α hypoxia response in tumor-infiltrating T lymphocytes induces functional CD137 (4-1BB) for immunotherapy. Cancer Discov 2012;2(7):608–23.
[25] Weigelin B, Bolaños E, Teijeira A, Martinez-Forero I, Labiano S, Azpilikueta A, et al. Focusing and sustaining the antitumor CTL effector killer response by agonist anti-CD137 mAb. PNAS 2015;112(24):7551–6.
[26] Fisher TS, Kamperschroer C, Oliphant T, Love VA, Lira PD, Doyonnas R, et al. Targeting of 4-1BB by monoclonal antibody PF-05082566 enhances T-cell function and promotes anti-tumor activity. Cancer Immunol Immunother 2012;61(10):1721–33.
[27] Topalian SL, Taube JM, Anders RA, Pardoll DM. Mechanism-driven biomarkers to guide immune checkpoint blockade in cancer therapy. Nat Rev Cancer 2016;16(5):275–87.

[28] Liu D, Schilling B, Liu D, Sucker A, Livingstone E, Jerby-Amon L, et al. Integrative molecular and clinical modeling of clinical outcomes to PD1 blockade in patients with metastatic melanoma. Nat Med 2019;25(12):1916–27.
[29] Durek P, Nordström K, Gasparoni G, Salhab A, Kressler C, de Almeida M, et al. Epigenomic profiling of human CD4+ T cells supports a linear differentiation model and highlights molecular regulators of memory development. Immunity 2016 15;45(5):1148–61.
[30] Ghoneim HE, Fan Y, Moustaki A, Abdelsamed HA, Dash P, Dogra P, et al. De novo epigenetic programs inhibit PD-1 blockade-mediated t cell rejuvenation. Cell 2017;170(1):142–57 e19.
[31] Scharer CD, Barwick BG, Youngblood BA, Ahmed R, Boss JM. Global DNA methylation remodeling accompanies CD8 T cell effector function. J Immunol 2013;191 (6):3419–29.
[32] Chen Y-P, Zhang J, Wang Y-Q, Liu N, He Q-M, Yang X-J, et al. The immune molecular landscape of the B7 and TNFR immunoregulatory ligand-receptor families in head and neck cancer: a comprehensive overview and the immunotherapeutic implications. Oncoimmunology 2017;6(3):e1288329.
[33] Gevensleben H, Holmes EE, Goltz D, Dietrich J, Sailer V, Ellinger J, et al. PD-L1 promoter methylation is a prognostic biomarker for biochemical recurrence-free survival in prostate cancer patients following radical prostatectomy. Oncotarget 2016;7(48):79943–55.
[34] Goltz D, Gevensleben H, Dietrich J, Ellinger J, Landsberg J, Kristiansen G, et al. Promoter methylation of the immune checkpoint receptor PD-1 (PDCD1) is an independent prognostic biomarker for biochemical recurrence-free survival in prostate cancer patients following radical prostatectomy. Oncoimmunology 2016;5(10):e1221555.
[35] Goltz D, Gevensleben H, Dietrich J, Schroeck F, de Vos L, Droege F, et al. PDCD1 (PD-1) promoter methylation predicts outcome in head and neck squamous cell carcinoma patients. Oncotarget 2017;8(25):41011–20.
[36] Goltz D, Gevensleben H, Dietrich J, Dietrich D. PD-L1 (CD274) promoter methylation predicts survival in colorectal cancer patients. Oncoimmunology 2017;6(1): e1257454.
[37] Goltz D, Gevensleben H, Grünen S, Dietrich J, Kristiansen G, Landsberg J, et al. PD-L1 (CD274) promoter methylation predicts survival in patients with acute myeloid leukemia. Leukemia 2017;31(3):738–43.
[38] Micevic G, Thakral D, McGeary M, Bosenberg M. PD-L1 methylation regulates PD-L1 expression and is associated with melanoma survival. Pigment Cell Melanoma Res 2019;32(3):435–40. doi: 10.1111/pcmr.12745.
[39] Röver LK, Gevensleben H, Dietrich J, Bootz F, Landsberg J, Goltz D, et al. PD-1 (PDCD1) promoter methylation is a prognostic factor in patients with diffuse lower-grade gliomas harboring isocitrate dehydrogenase (IDH) mutations. EBioMedicine 2018;28:97–104.
[40] Lingohr P, Dohmen J, Semaan A, Branchi V, Dietrich J, Bootz F, et al. Clinicopathological, immune and molecular correlates of PD-L2 methylation in gastric adenocarcinomas. Epigenomics 2019;11(6):639–53. doi: 10.2217/epi-2018-0149.
[41] Goltz D, Gevensleben H, Vogt TJ, Dietrich J, Golletz C, Bootz F, et al. CTLA4 methylation predicts response to anti-PD-1 and anti-CTLA-4 immunotherapy in melanoma patients. JCI Insight 2018;3(13):e96793.
[42] Ye Q, Song D-G, Poussin M, Yamamoto T, Best A, Li C, et al. CD137 accurately identifies and enriches for naturally-occurring tumor-reactive T cells in tumor. Clin Cancer Res 2014;20(1):44–55.
[43] Jacquelot N, Roberti MP, Enot DP, Rusakiewicz S, Ternès N, Jegou S, et al. Predictors of responses to immune checkpoint blockade in advanced melanoma. Nat Commun 2017;8(1):1–13.
[44] Jones PA. Functions of DNA methylation: islands, start sites, gene bodies and beyond. Nat Rev Genet 2012;13(7):484–92.
[45] Cancer Genome Atlas Network. Genomic classification of cutaneous melanoma. Cell 2015;161(7):1681–96.
[46] Thorsson V, Gibbs DL, Brown SD, Wolf D, Bortone DS, Ou Yang T-H, et al. The immune landscape of cancer. Immunity 2018;48(4):812–30 e14.
[47] Wu X, Zhang H, Xing Q, Cui J, Li J, Li Y, et al. PD-1(+) CD8(+) T cells are exhausted in tumours and functional in draining lymph nodes of colorectal cancer patients. Br J Cancer 2014;111(7):1391–9.
[48] Azimi F, Scolyer RA, Rumcheva P, Moncrieff M, Murali R, McCarthy SW, et al. Tumor-infiltrating lymphocyte grade is an independent predictor of sentinel lymph node status and survival in patients with cutaneous melanoma. J Clin Oncol 2012;30(21):2678–83.
[49] Youngblood B, Hale JS, Kissick HT, Ahn E, Xu X, Wieland A, et al. Effector CD8 T cells dedifferentiate into long-lived memory cells. Nature 2017;552(7685):404–9.
[50] Marwitz S, Scheufele S, Perner S, Reck M, Ammerpohl O, Goldmann T. Epigenetic modifications of the immune-checkpoint genes CTLA4 and PDCD1 in non-small cell lung cancer results in increased expression. Clin Epigenetics 2017;9:51.
[51] Choi BK, Lee SC, Lee MJ, Kim YH, Kim Y-W, Ryu K-W, et al. 4-1BB-based Isolation and expansion of CD8+ T cells specific for self-tumor and non-self-tumor antigens for adoptive T-cell therapy. J Immunother 2014;37(4):225.
[52] Melero I, Johnston JV, Shufford WW, Mittler RS, Chen L. NK1.1 cells express 4-1BB (CDw137) costimulatory molecule and are required for tumor immunity elicited by Anti-4-1BB monoclonal antibodies. Cell Immunol 1998;190(2):167–72.
[53] So T, Lee S-W, Croft M. Immune regulation and control of regulatory T cells by OX40 and 4-1BB. Cytokine Growth Factor Rev 2008;19(3–4):253–62.
[54] Lee S-W, Park Y, So T, Kwon BS, Cheroutre H, Mittler RS, et al. Identification of regulatory functions for 4-1BB and 4-1BBL in myelopoiesis and the development of dendritic cells. Nat Immunol 2008;9(8):917–26.
[55] Espinosa E, Márquez-Rodas I, Soria A, Berrocal A, Manzano JL, Gonzalez-Cao M, et al. Predictive factors of response to immunotherapy—a review from the Spanish Melanoma Group (GEM). Ann Transl Med 2017;5(19) [cited 2018 Oct 3]Available from: https://www.ncbi.nlm.nih.gov/pmc/articles/PMC5653511/.
[56] Vinay DS, Cha K, Kwon BS. Dual immunoregulatory pathways of 4-1BB signaling. J Mol Med 2006;84(9):726–36.
[57] Tolcher AW, Sznol M, Hu-Lieskovan S, Papadopoulos KP, Patnaik A, Rasco DW, et al. Phase IB study of utomilumab (PF-05082566), a 4-1BB/CD137 agonist, in combination with pembrolizumab (MK-3475) in patients with advanced solid tumors. Clin Cancer Res 2017;23(18):5349–57.
[58] Ni L, Lu J. Interferon gamma in cancer immunotherapy. Cancer Med 2018;7 (9):4509–16.
[59] Ayers M, Lunceford J, Nebozhyn M, Murphy E, Loboda A, Kaufman DR, et al. IFN-γ–related mRNA profile predicts clinical response to PD-1 blockade. J Clin Invest 2017;127(8):2930–40.
[60] Aznar MA, Labiano S, Diaz-Lagares A, Molina C, Garasa S, Azpilikueta A, et al. CD137 (4-1BB) costimulation modifies DNA methylation in CD8+ T cell-relevant genes. Cancer Immunol Res 2018;6(1):69–78.
[61] Hodis E, Watson IR, Kryukov GV, Arold ST, Imielinski M, Theurillat J-P, et al. A landscape of driver mutations in melanoma. Cell 2012;150(2):251–63.
[62] Parmenter TJ, Kleinschmidt M, Kinross KM, Bond ST, Li J, Kaadige MR, et al. Response of BRAF-mutant melanoma to BRAF inhibition is mediated by a network of transcriptional regulators of glycolysis. Cancer Discov 2014;4(4):423–33.
[63] Weisenberger DJ, Siegmund KD, Campan M, Young J, Long TI, Faasse MA, et al. CpG island methylator phenotype underlies sporadic microsatellite instability and is tightly associated with BRAF mutation in colorectal cancer. Nat Genet 2006;38(7):787–93.
[64] Jin S-G, Xiong W, Wu X, Yang L, Pfeifer GP. The DNA methylation landscape of human melanoma. Genomics 2015;106(6):322–30.
[65] Ilieva KM, Correa I, Josephs DH, Karagiannis P, Egbuniwe IU, Cafferkey MJ, et al. Effects of BRAF mutations and BRAF inhibition on immune responses to melanoma. Mol Cancer Ther 2014;13(12):2769–83.
[66] Amankulor NM, Kim Y, Arora S, Kargl J, Szulzewsky F, Hanke M, et al. Mutant IDH1 regulates the tumor-associated immune system in gliomas. Genes Dev 2017;31(8):774–86.
[67] Kim J, Kim K, Kim H, Yoon G, Lee K. Characterization of age signatures of DNA methylation in normal and cancer tissues from multiple studies. BMC Genom 2014;15:997.
[68] Peters MJ, Joehanes R, Pilling LC, Schurmann C, Conneely KN, Powell J, et al. The transcriptional landscape of age in human peripheral blood. Nat Commun 2015;6:8570.
[69] Acevedo N, Reinius LE, Vitezic M, Fortino V, Söderhäll C, Honkanen H, et al. Age-associated DNA methylation changes in immune genes, histone modifiers and chromatin remodeling factors within 5 years after birth in human blood leukocytes. Clin Epigenetics 2015;7:34.
[70] Dozmorov MG, Coit P, Maksimowicz-McKinnon K, Sawalha AH. Age-associated DNA methylation changes in naive CD4+ T cells suggest an evolving autoimmune epigenotype in aging T cells. Epigenomics 2017;9(4):429–45.
[71] Tserel L, Kolde R, Limbach M, Tretyakov K, Kasela S, Kisand K, et al. Age-related profiling of DNA methylation in CD8+ T cells reveals changes in immune response and transcriptional regulator genes. Sci Rep 2015;5:13107.
[72] Steegenga WT, Boekschoten MV, Lute C, Hooiveld GJ, de Groot PJ, Morris TJ, et al. Genome-wide age-related changes in DNA methylation and gene expression in human PBMCs. Age 2014;36(3):9648.
[73] Carter SL, Cibulskis K, Helman E, McKenna A, Shen H, Zack T, et al. Absolute quantification of somatic DNA alterations in human cancer. Nat Biotechnol 2012;30 (5):413–21.
[74] Saltz J, Gupta R, Hou L, Kurc T, Singh P, Nguyen V, et al. Spatial organization and molecular correlation of tumor-infiltrating lymphocytes using deep learning on pathology images. Cell Rep 2018;23(1):181–93 e7.
[75] Newman AM, Liu CL, Green MR, Gentles AJ, Feng W, Xu Y, et al. Robust enumeration of cell subsets from tissue expression profiles. Nat Methods 2015;12(5):453–7.
[76] Edgar R, Domrachev M, Lash AE. Gene expression omnibus: NCBI gene expression and hybridization array data repository. Nucleic Acids Res 2002;30(1):207–10.
[77] Barrett T, Wilhite SE, Ledoux P, Evangelista C, Kim IF, Tomashevsky M, et al. NCBI GEO: archive for functional genomics data sets—update. Nucleic Acids Res 2013;41(Database issue):D991–5.
[78] Marzese DM, Scolyer RA, Huynh JL, Huang SK, Hirose H, Chong KK, et al. Epigenome-wide DNA methylation landscape of melanoma progression to brain metastasis reveals aberrations on homeobox D cluster associated with prognosis. Hum Mol Genet 2014;23(1):226–38.
[79] Fujiwara S, Nagai H, Jimbo H, Jimbo N, Tanaka T, Inoie M, et al. Gene expression and methylation analysis in melanomas and melanocytes from the same patient: loss of NPM2 expression is a potential immunohistochemical marker for melanoma. Front Oncol 2018;8:675.
[80] Zhu H, Mi W, Luo H, Chen T, Liu S, Raman I, et al. Whole-genome transcription and DNA methylation analysis of peripheral blood mononuclear cells identified aberrant gene regulation pathways in systemic lupus erythematosus. Arthritis Res Ther 2016;18:162. 13.
[81] Mamrut S, Avidan N, Staun-Ram E, Ginzburg E, Truffault F, Berrih-Aknin S, et al. Integrative analysis of methylome and transcriptome in human blood identifies extensive sex- and immune cell-specific differentially methylated regions. Epigenetics 2015;10(10):943–57.

[82] Ventham NT, Kennedy NA, Adams AT, Kalla R, Heath S, O'Leary KR, et al. Integrative epigenome-wide analysis demonstrates that DNA methylation may mediate genetic risk in inflammatory bowel disease. Nat Commun 2016;7:13507. 25.
[83] Absher DM, Li X, Waite LL, Gibson A, Roberts K, Edberg J, et al. Genome-wide DNA methylation analysis of systemic lupus erythematosus reveals persistent hypomethylation of interferon genes and compositional changes to CD4+ T-cell populations. PLoS Genet 2013;9(8):e1003678.
[84] Li B, Dewey CN. RSEM: accurate transcript quantification from RNA-Seq data with or without a reference genome. BMC Bioinform 2011;12:323.
[85] Du P, Zhang X, Huang C-C, Jafari N, Kibbe WA, Hou L, et al. Comparison of Beta-value and M-value methods for quantifying methylation levels by microarray analysis. BMC Bioinform 2010;11:587.
[86] Lehmann U, Kreipe H. Real-time PCR-based assay for quantitative determination of methylation status. Methods Mol Biol 2004;287:207–18.
[87] Zerbino DR, Achuthan P, Akanni W, Amode MR, Barrell D, Bhai J, et al. Ensembl 2018. Nucleic Acids Res 2018;46(D1):D754–61.
[88] Jung M, Uhl B, Kristiansen G, Dietrich D. Bisulfite conversion of DNA from tissues, cell lines, buffy coat, FFPE tissues, microdissected cells, swabs, sputum, aspirates, lavages, effusions, plasma, serum, and urine. Methods Mol Biol 2017;1589:139–59.